UNIVERSITI PUTRA MALAYSIA

DEVELOPMENT OF GG-DMSO-LiI-I2 GEL POLYMER ELECTROLYTES FOR POTENTIAL DYE SENSITIZED SOLAR CELL APPLICATION

MUHAMMAD AKMAL HAKEEM BIN MOHD IRMAN

DEVELOPMENT OF GG-DMSO-LiI-I_2 GEL POLYMER ELECTROLYTES FOR POTENTIAL DYE SENSITIZED SOLAR CELL APPLICATION

By

MUHAMMAD AKMAL HAKEEM BIN MOHD IRMAN

Thesis Submitted to the Department of Physics, Universiti Putra Malaysia, in partial Fulfilment of the Requirements for the Bachelor of Science in Materials Science with Honours

February 2022

DEDICATION

To my beloved parents

Mohd Irman bin Mohd Arsan and Roslina binti Mohd Tarmizi
who has always taught me to trust in Allah and believe in hard work. My parents always been a source of my motivation and strength during the moments of despair and discouragement and give their endless love, support and encouragement throughout my life.

To my respected supervisor

Dr. Ikhwan Syafiq bin Mohd Noor
who shows me his compassionate consistent cooperation and guidance to me to complete this project successfully and always advise me about future career and life.

To my lecturers and teachers

Who shows their sincere guidance and always teach me new knowledge and experiences in and out of the classroom.

To my lovely siblings

Rozeen, Naeem, Muneer and Faheem
who always be there for me during the time I need them most and taught me to be a responsible and reliable brother.

To my dearest friends

Nik Muhammad Azamuddin bin Che Daud, Muhamad Izzat bin Mohd Azmi and my best friends who always support behind my back and helped me a lot during this university life and to make this project a success.

ABSTRACT

DEVELOPMENT OF GG-DMSO-LiI-I_2 GEL POLYMER ELECTROLYTES FOR POTENTIAL DYE SENSITIZED SOLAR CELL APPLICATION

By

Muhammad Akmal Hakeem Bin Mohd Irman

198803

February 2022

Supervisor: Dr. Ikhwan Syafiq Bin Mohd Noor

Faculty: Faculty of Science

Dye sensitized solar cells (DSSCs) have recently gain attention due to their high solar energy efficiency, low cost, and simple production techniques. Because of these advantageous, DSSCs have been proposed as an innovative replacement for current conventional silicon solar cells. Polymer electrolytes are commonly used as a charge transfer medium in DSSCs. However, polymer electrolytes are based on synthetic polymers that are not eco-friendly. Biopolymers are actively studied in order to replace synthetic polymers as base materials in polymer electrolytes. In this work, gellan gum (GG) biopolymer is employed as a host to prepare gel polymer electrolyte (GPEs). Lithium iodide (LiI) and iodide (I_2) salts act as charge carrier supplies. DMSO was added to form a gel-state electrolyte. Two electrolyte systems were prepared which are DMSO-LiI-I_2 liquid electrolytes (system 1) and GG-DMSO-LiI-I_2 GPEs (system 2). For system 1, electrolyte with 87.36 wt.% DMSO-10.63 wt.% LiI-2.02 wt.% I_2 (LA electrolyte) revealed the highest ionic conductivity (σ) of (10.89±0.45) mS cm^{-1} at room temperature. The highest σ value obtained by the LA3 electrolyte is

largely controlled by the charge carrier concentration (n) relative to the mobility (μ). Since the LA3 electrolyte has the highest σ, various amount of gellan gum (GG) was added into this electrolyte composition to form GPEs (system 2). GPE of 5.50 wt.% GG-82.55 wt.% DMSO-10.05 wt.% LiI-1.90 wt.% I_2 (GA2 electrolyte) showed the highest σ of 7.63 mS cm^{-1} at room temperature. High room temperature σ was highly influence by high μ relative to n. The conductivity-temperature study shows that conductivity increased with temperature increased, controlled by the increased in n, not μ. All GPEs in system 2 was fabricated in DSSC. The DSSC with GA2 electrolyte revealed the highest power conversion efficiency (PCE) of (2.15±0.01) % along with highest short circuit current (J_{sc}) of (4.79±0.01) mA cm^{-2}, impact from the highest σ_{rt} due to high μ relative to n, which facilitated the redox process in DSSC. The highest J_{sc} of DSSC was supported by the lowest charge transfer resistance (R_{ct}) of 36.5 Ω. Based on this work, it can be concluded that biopolymer GG-based GPEs have great potential for use in DSSC applications.

ABSTRAK

PEMBANGUNAN GG-DMSO-LiI-I_2 ELEKTROLIT POLIMER GEL UNTUK APLIKASI SEL SURIA TERPEKA PEWARNA

Oleh

Muhammad Akmal Hakeem Bin Mohd Irman

198803

Februari 2022

Penyelia: Dr. Ikhwan Syafiq Bin Mohd Noor

Fakulti: Fakulti Sains

Sel suria pemeka pewarna (DSSC) kebelakangan ini mendapat perhatian kerana kecekapan tenaga suria yang tinggi, kos rendah dan teknik pengeluaran yang mudah. Kerana kelebihan ini, DSSC telah dicadangkan sebagai pengganti inovatif untuk sel suria silikon konvensional semasa. Elektrolit polimer biasanya digunakan sebagai medium pemindahan cas dalam DSSC. Namun, elektrolit polimer adalah berasaskan polimer sintetik yang tidak mesra alam. Biopolimer dikaji secara aktif untuk menggantikan polimer sintetik sebagai bahan asas dalam elektrolit polimer. Dalam kerja ini, biopolimer gellan gum (GG) digunakan sebagai perumah untuk menyediakan elektrolit polimer gel (EPG). Garam litium iodida (LiI) dan iodida (I_2) bertindak sebagai bekalan pembawa cas. DMSO telah ditambah untuk membentuk elektrolit keadaan gel. Dua sistem elektrolit telah disediakan iaitu elektrolit cecair DMSO-LiI-I_2 (sistem 1) dan GG-DMSO-LiI-I_2 EPG (sistem 2). Untuk sistem 1, elektrolit dengan 87.36 wt.% DMSO-10.63 wt.% LiI-2.02 wt.% I_2 mendedahkan kekonduksian ionik (σ) tertinggi iaitu (10.89±0.45) mS cm^{-1} pada suhu bilik. Nilai σ

tertinggi yang diperolehi oleh elektrolit GI2 dipengaruhi oleh kedua-dua *n* dan μ. Oleh kerana elektrolit LA3 mempunyai σ tertinggi, jumlah berbeza gellan gum (GG) telah ditambah ke dalam komposisi elektrolit ini untuk membentuk EPG (sistem 2). EPG dengan 5.50 wt.% GG-82.55 wt.% DMSO-10.05 wt.% LiI-1.90 wt.% I_2 (GA2 elektrolit) menunjukkan σ tertinggi iaitu 7.63 mS cm^{-1} pada suhu bilik. Nilai σ pada suhu bilik sangat dipengaruhi oleh μ yang tinggi berbanding *n*. Kajian kekonduksian-suhu menunjukkan bahawa kekonduksian meningkat dengan peningkatan suhu, dikawal oleh peningkatan dalam *n*, bukan μ. Semua EPG dalam sistem 2 telah dipasang dalam DSSC. DSSC dengan elektrolit GA2 mendedahkan kecekapan penukaran tenaga (KPT) tertinggi iaitu (2.15±0.01) % seiring dengan arus litar pintas (J_{sc}) tertinggi iaitu (4.79±0.01) mA cm^{-2}, kesan dari σ tertinggi disebabkan oleh μ yang tinggi berbanding *n*, yang memudahkan proses redoks dalam DSSC. J_{sc} tertinggi DSSC disokong oleh rintangan pemindahan cas (R_{ct}) terendah sebanyak 36.5 Ω. Berdasarkan kerja ini, dapat disimpulkan bahawa EPG berasaskan GG biopolymer mempunyai potensi besar untuk digunakan dalam aplikasi DSSC.

ACKNOWLEDGEMENT

This research project has allowed me to learn and gain knowledge that has personally and professionally shaped me into a better person. I would like to take this opportunity to express my gratitude to everyone that contributed a great amount of assistance to me until I successfully complete this thesis.

First and foremost, I would like to express my deepest appreciation to my supervisor, Dr Ikhwan Syafiq Mohd Noor who is patiently provide guidance and motivation to me throughout the duration of this project. His dedication, insightful suggestion as well as his profound belief in my abilities have helped me in a lot of ways upon completing our final project.

Next, I would like to extend my sincere thanks to Universiti Putra Malaysia that provided the facilities, well-equipped apparatus and equipment to be utilised in this work. Special thanks to Centre for Ionics, University Malaya for providing technical assistance in characterizing the samples.

Other than that, I am also grateful to my friends and coursemates who were always supporting me in the journey of completing this work. I would like to thank them for kindly sharing any information or knowledge with me.

Last but not least, I wish to extend my gratitude to my beloved family that provide unrelenting physical and moral support and great love towards me. This project would not be possible without their unwavering support and motivation.

Date: ……..……

Assoc. Prof. Dr. Suriati Paiman

Head of Department

Department of Physics

Faculty of Science

Universiti Putra Malaysia

Table of Content

LIST OF FIGURES

LIST OF TABLES

LIST OF ABBREVIATIONS

DSSC	Dye sensitized solar cell
PE	Polymer electrolyte
GPE	Gel polymer electrolyte
SPE	Solid polymer electrolyte
CPE	Composite polymer electrolyte
EIS	Electrical Impedance Spectroscopy
FTO	Fluorine-doped tin oxide
I_2	Iodine
GG	Gellan gum
LiI	Lithium iodide
DMSO	Dimethyl sulfoxide
wt.%	Weight percent
Z'	Real impedance
Z''	Imaginary impedance
σ	Ionic conductivity
n	Number density of charge carrier
μ	Mobility of charge carrier
D	Diffusion coefficient of charge carrier
J_{sc}	Short current density
V_{oc}	Voltage open circuit
FF	Fill factor
PCE	Power conversion efficiency
R_{ct}	Charge transfer resistance

CHAPTER 1

INTRODUCTION

1.1 Introduction

Dye sensitized solar cells (DSSCs) have gained acknowledgement as a prominent suitable alternative to the latest silicon solar cells due to its simplicity, effectiveness and maximizing the use of affordable and naturally plentiful materials (Arof *et al.*, 2017; Colovic *et al.*, 2019; Shah *et al.*, 2017; Su'ait *et al.*, 2015). Latest studies revealed that DSSCs have current efficiencies up to 14.3% and 14.7% when exposed respectively under 100 mW cm^{-2} and 50 mW cm^{-2} light intensity (Kakiage *et al.*, 2015). The cell was fabricated with electrolyte made of 0.20 M $[Co^{2+}(phen)_3](PF_6^-)_2$, 0.05 M $[Co^{3+}(phen)_3](PF_6^-)_3$, 0.07 M $LiClO_4$, 0.02 M $NaClO_4$, 0.03 M TBAPF, 0. 01 M TBPPF, 0.01 MHMImPF, 0.30 M TBP, 0.10 M TMSP, 0.10 M MP, 0.05 M CPrBP, 0.10 M CPeBP, and 0.05 MCOcBP in MeCN) sandwiched between TiO_2/LEG4/ADEKA-1 photoanode and Au/GNP counter electrode. In comparison, the conventional silicon-based solar cell has achieved efficiencies of up to 27.8% in the laboratory (Köhnen *et al.*, 2021), with a theoretical maximum efficiency of 46.0% (*Köhnen et al.*, 2021). Based on this latest discovery, it is believed that DSSC will be a reliable energy harvesting technology that will be eventually replacing traditional silicon-based solar cells (Chowdhury *et al.*, 2020). The DSSC structure comprises primarily of an electrolyte sandwiched between a dye/metal-oxide semiconductor photoanode that serves as a working electrode and a counter electrode (mostly used platinum). The dyes at the photoanode operates as a light absorber, allowing electrons to be generated. Electrolyte is one of the crucial components to

understand in DSSCs since it acts as a medium for the electrons transfer from the counter electrode to the ionized dyes at the working electrode. Excellent DSSC performance will be achieved with a good electrolyte. Therefore, an electrolyte with excellent characteristics is sought in this study to increase the DSSC efficiency.

1.2 Problem Statement

Electrolyte is one of the most important materials in DSSC applications. It acts as a charge carriers' medium from the counter electrode to the ionizing dye on the working electrode. Liquid electrolytes are more typically utilized in DSSC due to its high ionic conductivity. Nevertheless, liquid electrolytes a number of major drawback including leakage, volatility, easy desorption and evaporation, flammable, and easy to corrode the counter electrode in DSSC (Abdukarimov *et al.*, 2020; Arof *et al.*, 2017; Chowdhury *et al.*, 2020; Venkatesan *et al.*, 2019; Yun *et al.*, 2014; Zhang *et al.*, 2015). Polymer electrolyte has become a priority, and it is currently commonly employed as a redox material in DSSCs because of its advantageous of flexibility in size and stability, lightweight, ease of formation, non-leakiness, and good electrode-electrolyte contact (Arya & Sharma, 2017).

Polymer electrolytes can be categorized into three groups which are synthetic polymers, semi-synthetic polymers and biopolymer. Most synthetic polymers commonly used as base materials in polymer electrolytes and applied in electrochemical devices especially DSSCs. Polyethylene oxide (PEO), polyacrylonitrile (PAN), polyethylene glycol (PEG), polyvinyl pyrrolidine (PVP), polyethylene (PE), polystyrene (PS), polyamides (nylon), polyvinyl chloride (PVC), synthetic rubber, Teflon and epoxy are the examples of synthetic polymers (Arof *et al.*, 2017; Verma *et al.*, 2010). Synthetic polymers are known to have many

disadvantages such as their high toxicity and non-economic value (Bharadwaz & Jayasuriya, 2020; Neto *et al.*, 2015). Biopolymers are the materials made from microorganisms that live in the environment (Singh *et al.*, 2013). Their natural abundance, low cost, and green characteristics make it a good fit to replace synthetic polymer as base materials in polymer electrolytes (Bharadwaz & Jayasuriya, 2020; Neto *et al.*, 2015; I. S. M. Noor *et al.*, 2012). Many studies are being actively conducted to develop biopolymer-based electrolyte and used in electrochemical devices including DSSCs.

In this work, gellan gum (GG) biopolymer will be used as a host polymer for gel polymer electrolytes (GPEs). Lithium iodide (LiI) and iodine (I_2) salts were selected as charge suppliers to generate redox process. It is reported that the iodide/triiodide (I^-/I_3^-) redox couple has good solubility, does not absorb too much light, has a suitable redox potential, and provides rapid dye regeneration, making it an option redox material for this work. Besides, (I^-/I_3^-) redox couple is reported to reveal high power conversion efficiency since the energy may be matched with the sensitized dye, and it has a naturally high diffusion coefficient in the electrolyte (Suhaimi *et al.*, 2015). In this work, gel polymer electrolytes (GPEs) will be produced. GPEs have significantly greater ionic conductivity than a solid polymer electrolyte and higher reliability than a liquid electrolyte. To form a gel-type electrolyte, dimethyl sulfoxide (DMSO) will be used as the solvent.

1.3 Objective of Study

Based on the problem statements, this project was designed in order to expand knowledge. The objectives for this study are:

i. to produce a new gel polymer electrolyte based on GG-DMSO-LiI-I_2 complexes.

ii. to evaluate the dynamic ion properties in GG-DMSO-LiI-I_2 gel polymer electrolyte at room and elevated temperature.

iii. to test the potential of GG-DMSO-LiI-I_2 gel polymer electrolytes in dye sensitized solar cells.

1.4 Thesis Outline

This thesis consists of five chapters. The first chapter includes an introduction to the scope of the study. The problem statement and the objectives of this work are also addressed in the first chapter.

Chapter 2 generally states a literature review of solar cells, polymer electrolytes, and the materials selected for this work.

The method to prepare the gel polymer electrolytes (GPEs) are explained in Chapter 3. The procedure for electrical impedance spectroscopy (EIS) characterization, fabrication, and characterization of DSSCs are also explained in this chapter.

In Chapter 4, the data and results obtained from the EIS and DSSC photovoltaic characteristics are analyzed and discussed in further detailed.

Lastly, the conclusion of this study is presented in Chapter 5. The suggestions for future research also expressed in Chapter 5.

CHAPTER 2

LITERATURE REVIEW

2.1 Introduction

This chapter covers the background studies that are related to this project. The concept of solar cells, dye sensitized solar cells (DSSCs), polymer, polymer electrolyte, gellan gum (GG), dimethyl sulfoxide (DMSO), lithium iodide (LiI) and iodine (I_2) are explained.

2.2 Solar Cell

Solar energy is one of the most abundant energies that will never run out. It is one of the renewable energy similar to wind, biomass and other energy that originated from renewable resources. It is undoubted that solar energy is the uttermost pure source of energy because it from the sun which cannot be destroyed or polluted (Moore & Wei, 2021).

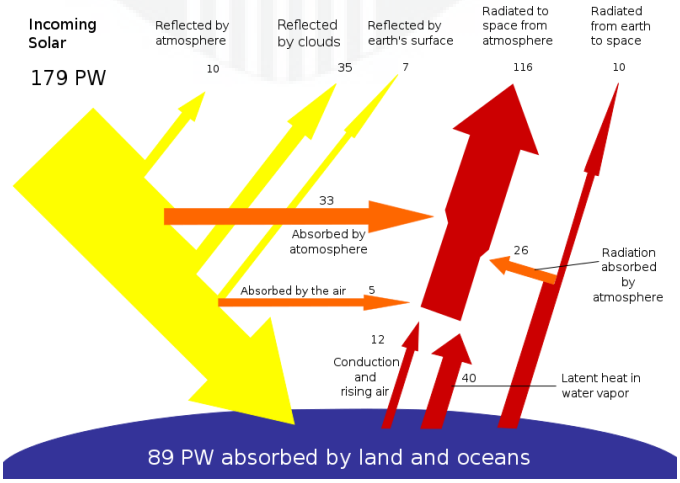

Figure 2.1. Schematic diagram of solar energy

Scientists have developed a device known as a solar cell that allows them to harness solar energy. Solar cells were first recognized in 1839 by French physicist named Edmond Becquerel in his father's laboratory. The first solid state photovoltaic cell was physically fabricated by Charles Fritts in 1883 with semiconductor selenium is coated with thin layer of gold. In the recent year, a lot of research has been done to improve solar cells specially to increase the efficiency of this device.

Solar cell is an invention that are specifically fabricated to convert the solar energy into the electrical energy through the effect of photovoltaic (N. Suresh Kumar & K. Chandra Babu Naidu, 2021). The three basic features are necessary in the operating mode of a solar cell are:

i. the absorption of light, producing either electron-hole pairs or excitons.

ii. the separation of charge carriers of opposite types.

iii. the separate extraction of the carrier to the external circuit.

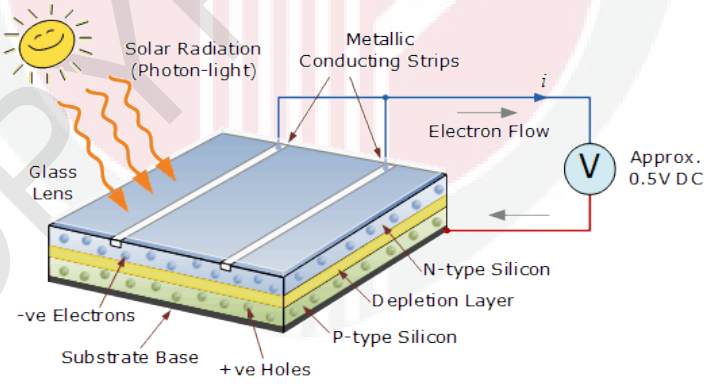

Figure 2.2. Schematic diagram of solar cell converting solar energy to electrical energy

Solar cell can be categorized into three different classes which are first-generation, second-generation and third-generation. Fundamentally, the first-generation solar cells are structured in the form of silicon-based wafer, which has the highest current efficiency of 27.8% among all solar cell generations. The second-

generation solar cells are constructed of thin film silicon and has a current efficiency of 23.4%, making it the most efficient solar cell currently available in the market. The third-generation solar cells are the most recent technology of photovoltaic cell that uses dyes as the light absorber and has a high current efficiency of 14.7%.

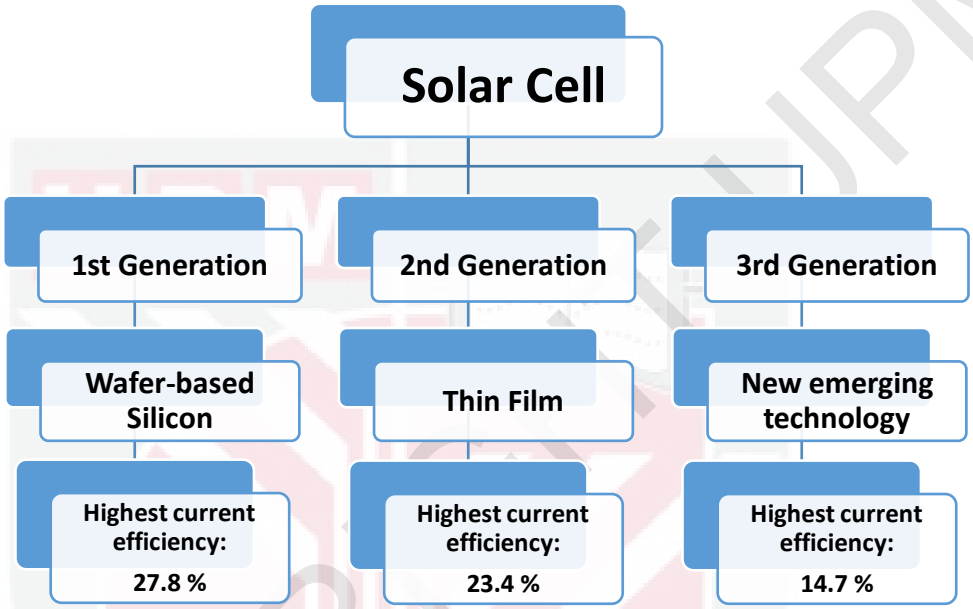

Figure 2.3. Solar cell classification

2.3 Dye Sensitized Solar Cell (DSSC)

Dye-sensitized solar cells (DSSCs) are one of the thin-film photovoltaic cells from the third-generation group. It was first introduced in 1991 by Oregan and Gratzel with a photoelectric conversion rate of 7.1%. The DSSC is composed of simple components such as sensitizer, metal oxide semiconductor (working electrode), a counter electrode (CE) and an electrolyte. These components are enough to spark the interest of researchers to investigate ways to improve the efficiencies of the DSSCs (Devadiga *et al.*, 2021). DSSCs was invented in order to replace the traditional silicon

solar cells that are known to have drawbacks such as high toxicity and are expensive. The advantages of DSSCs are:

- it is eco-friendly and translucent due to the materials characteristics itself (Su'ait *et al.*, 2015).
- it has relatively high energy conversion efficiency (up to 13%) (Careem *et al.*, 2017; Hassan *et al.*, 2014).
- low production cost (Upadhyaya *et al.*, 2013).
- easy and simple to fabricate (Chowdhury *et al.*, 2020).

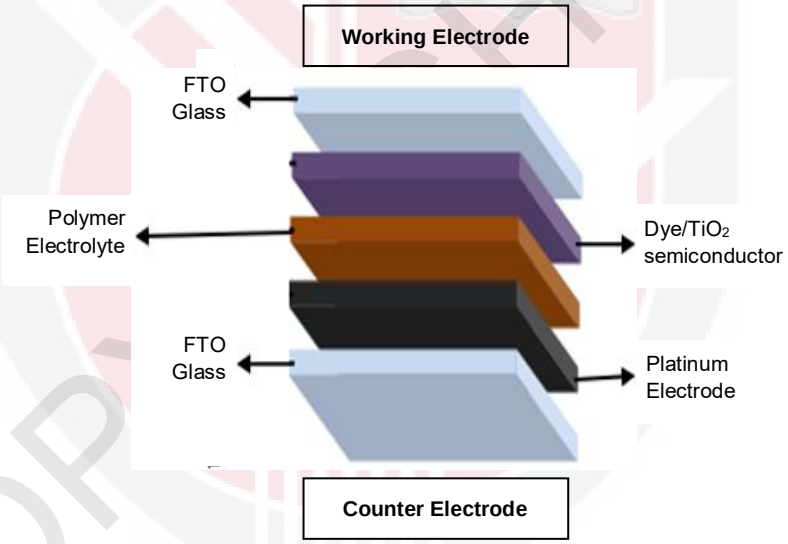

Figure 2.4. Structure of DSSC

In DSSC, two primary electrodes which are a photoanode (working electrode) and a counter electrode sandwiching the electrolytes containing redox mediators. The electrolytes separating both electrodes are mostly composed of iodide (I^-) ion. Electrolytes play a vital role in transferring charge from the counter electrode to the photoanode.

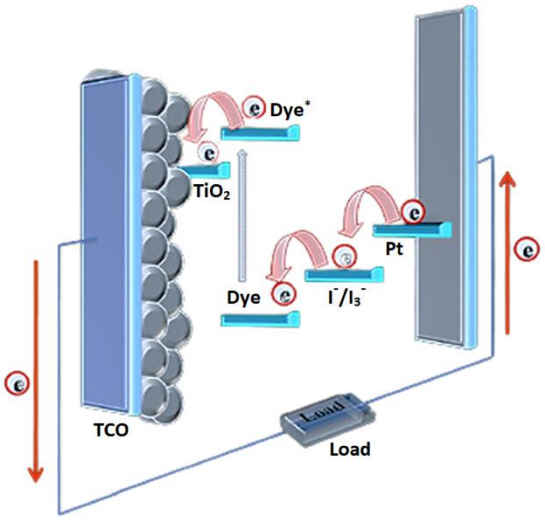

Figure 2.5. Schematic diagram of DSSC

DSSC has simple mechanisms to generate electricity from the solar energy. Referring to Figure 2.5, the DSSCs mechanism can be divided into several important parts. It begins when the dyes absorb photons coming from sunlight. The dyes then excite from a ground state to the excited state and releases electrons (e^-). The dyes at the excited state are now the ionized dyes. The injected electrons then jump into the conduction band of titanium oxide (TiO_2) and pass through the photoanode to the external circuit. The electrons then continue to flow to the counter electrode. The I^- ions in the electrolyte then combine with electrons and are oxidized to I_3^- ions at the counter electrode. The I_3^- ion then travel from the counter electrode to the photoanode to transfer the electrons to the ionized dye and reduce to I^- ions. This process is cycle in order to maintain the functionality of the DSSCs.

2.4 Polymer

Polymer is a big molecule composed of small repeating units called monomers that are linked together by covalent bonds. Polymerization is a chemical reaction that

combines monomers to produce a polymer chain. Polymers are made up of long and complex chains of molecules and having a high molecular weight. Polymers can be categorized into three different types which are synthetic polymers, semi-synthetic polymers and biopolymers.

Synthetic polymers are the type of polymers that manufactured by the researchers in laboratories by synthesizing petroleum-based materials (Greek & War, 2018). It is often found in the medical field such as medical implant devices and drug delivery systems (Zainudin *et al.*, 2020). Semi-synthetic polymers are polymers developed from natural polymer that has been chemically modified. Poly(vinyl chloride), polyester, polystyrene, and polypropylene are the example of semi-synthetic polymers (Greek & War, 2018). Biopolymer are made from living things such as plants, animals and other organisms. It has many advantages over other types of polymers due to its properties of ow cost, environmental-friendly and natural abundance (Noor *et al.*, 2012). Due to these advantages, researchers around the world are actively using biopolymer extensively in their studies. Chitosan (Praveen *et al.*, 2020), agarose (Singh *et al.*, 2013), phytagel (Singh *et al.*, 2015), cellulose (Li *et al.*, 2011), and gellan gum (Noor, 2020) are the examples of biopolymers being actively studied.

2.5 Polymer Electrolyte

Polymer electrolytes are the materials that can conduct ions formed from dissolution of an inorganic salts into a suitable polymer that acts as a host. Polymer electrolytes can be classified into three group which are solid polymer electrolytes, composite polymer electrolytes and gel polymer electrolytes (Arya & Sharma, 2017). Each type of the polymer electrolyte has its own functions and advantages.

Solid polymer electrolyte (SPE) is formed by incorporating inorganic salt into a polar polymer, resulting in an ion conducting electrolyte (Edman *et al.*, 2000). The electrostatic interaction of salt metal ions with polar polymers leads in the formation of a coordination bond (Rivas *et al.*, 2008). Ions begin to migrate from one coordination site to another when the polymer electrolyte is subjected to an electric field. This situation occurred due to a weaker contact between the metal ion and the functional group of the polymer chain. Solid polymer electrolytes are high flexible and thermally, mechanically, and chemically stabile. Unfortunately, this type of electrolyte has low ionic conductivity (~10^{-4} S cm^{-1}).

Composite polymer electrolytes (CPEs) are produced in order to overcome the conductivity limit in SPEs. Less number of ion dissociation due to low dielectric constant of polymer host causes the SPEs conductivity to be lower (Mohapatra *et al.*, 2009). CPEs are made up of a combination of polymer electrolytes with inorganic inert fillers such as TiO_2, SiO_2 and Al_2O_3 that helps increase the dissociation of salt ions in polymer electrolytes (Mulmi *et al.*, 2009). The CPEs have good properties of high conductivity as well as thermally, mechanically and chemically stable.

Gel polymer electrolytes (GPEs) are the polymer electrolytes that are in semi-solid state. It was developed to overcome the limitations that occur in liquid electrolytes and solid polymer electrolytes. Fundamentally, GPEs are the combination of liquid electrolytes and solid polymer electrolytes that combines the important advantages of these two electrolyte types into one electrolyte. GPEs is now a hot topic in research because of its advantages of:

- providing high ionic conductivity (10^{-3} S cm^{-1}) (Arya & Sharma, 2017).
- non-flammable (Arof *et al.*, 2017).
- improving electrode/electrolyte contact (Arof *et al.*, 2017).

- not producing harmful gases (Arya & Sharma, 2017).
- non-leak (Arya & Sharma, 2017).

Currently, GPEs being the most favourable electrolytes to use in DSSCs. This is because it can reveal high power conversion efficiency (PCE) when fabricated in DSSCs. Table 2.1 listed the examples of GPEs with corresponding ionic conductivity and DSSC PCE obtained from literatures.

Table 2.1. Examples of gel polymer electrolytes (GPEs) with corresponding ionic conductivity and DSSC power conversion efficiency (PCE)

GPE	σ_{RT} (S cm^{-1})	PCE (%)
8 wt.% PAN–30 wt.% EC–30 wt.% PC–30 wt.% TBAI–2 wt.% I_2 (Chowdhury *et al.*, 2020)	5.14×10^{-3}	3.45
56.78 wt.% P(VB-co-VA-co-Vac) –39.98 wt.% TPAI–3.24 wt.% I_2 (Farhana *et al.*, 2019)	4.16×10^{-3}	4.62
9.86 wt.% PAN–40.93 wt.% EC–37.97 wt.% PC–4.37 wt.% TPAI–1.24 wt.% BMII–4.35 wt.% LiI–1.28 wt.% I_2 (Arof *et al.*, 2017)	3.91×10^{-3}	5.40
5.62 wt.% PEO–5.62 wt.% PVA–24.08 wt.% DMSO–24.08 wt.% EC–19.27 wt.% TBAI–1.33 wt.% I_2–20 wt.% BMII (Sri *et al.*, 2017)	8.39×10^{-3}	7.49
4.37 wt.% PhCh–1.09 wt.% PEO–27.29 wt.% EC–32.75 wt.% DMF-24.66 wt.% TPAI–1.85 wt.% I_2–8 wt.% BMII (Buraidah *et al.*, 2017)	13.5×10^{-3}	9.61

Most of the GPEs used in DSSCs are synthetic-based polymers. Synthetic polymers are known for their high toxicity and are not environmentally friendly. The use of biopolymers as based materials in GPEs is now a concern as an alternative to synthetic polymers. Several reports as listed in Table 2.2. showed that the use of biopolymer-based GPEs in DSSC applications revealed an affordable PCE. This suggests that biopolymers have a great potential to replace synthetic polymers in GPEs and function well in DSSCs.

Table 2.2. DSSCs performance using gel polymer electrolytes based biopolymer

GPE	σ_{RT} (S cm^{-1})	PCE (%)
67.94 wt.% PUA–30 wt.% TBAI–2.06 wt.% I_2 (Chai *et al.*, 2020)	1.88×10^{-4}	1.97
15.44 wt.% PhSt–6.62 wt.% HEC–66.15 wt.% DMF–9.92 wt.% LiI–1.87 wt.% I_2 (Selvanathan *et al.*, 2020)	5.50×10^{-3}	3.67
15.7 wt.% PhCh–31.7 wt.% EC–31.7 wt.% PC–19wt.% TPAI–1.9 wt.% I_2 (Yusuf, *et al.*, 2014)	5.27×10^{-3}	3.71
14.95 wt.% PhSt–6.41 wt.% HEC–64.07 wt.% DMF-12.28 wt.% TPAI–2.3 wt.% I_2 (Selvanathan *et al.*, 2020)	4.97×10^{-3}	3.94

2.6 Gellan Gum (GG)

Gellan gum (GG) is a biopolymer that is made of 1,4-α-L-rhamnose, 1,3-β-D-glucose, 1,4-β-D-glucose and 1,4-β-D-glucuronic. It is belonging to a microbial polysaccharide group (Liu *et al.*, 2020). GG is a water-soluble anionic polysaccharide produced by fermentation of a carbohydrate by a bacteria known as *Pseudomonas elodea* (Noor, 2020; Neto *et al.*, 2015). Therefore, it can produce a strong gel due to the presence of polysaccharides which are the main structural component of algae cell walls (Singh *et al.*, 2015).

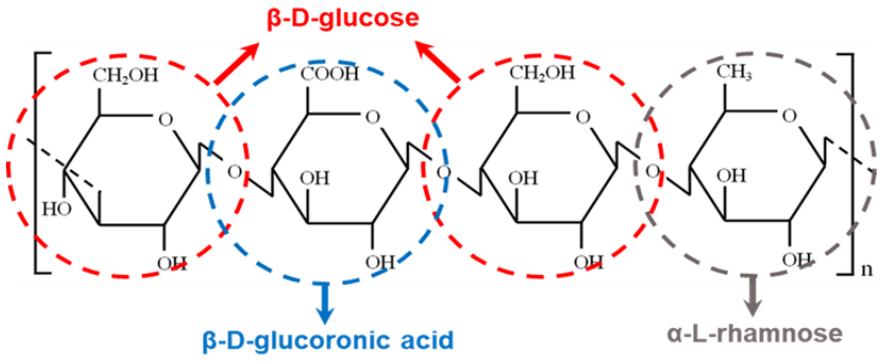

Figure 2.6. Chemical structure of gellan gum

GG containing the repetitive units of tetrasaccharide long chains composed of alpha-L-rhamnose, beta-D-glucose, and beta-D-glucuronic acid (I. M. Noor, 2020; I. S. M. Noor *et al.*, 2012). The chemical structure consists of a carboxyl group (COOH), an ether group and a hydroxyl group (OH) where it can provide more excess electrons to its structure allowing it to attract the free ions from dissociated salts (see Figure 2.6). The excess electrons on its heteroatoms provide a platform for cations from the salt to coordinate with its structure. GG has many good features which are (I. M. Noor, 2020; Singh *et al.*, 2015; Neto *et al.*, 2015; I. S. M. Noor *et al.*, 2012):

- high dielectric constant (ε_r = 6.7).
- able to produce high ionic conductivity (up to 10^{-4} S cm^{-1}).
- high thermal stability and reversibility (can perform valuable temperature).
- good mechanical strength.
- low cost.
- nontoxic.
- environmentally friendly.
- safe.
- Easy to degrade.

2.7 Dimethyl Sulfoxide (DMSO)

Dimethyl sulfoxide (DMSO) is an organosulfur compound that is highly polar organic liquid. It plays the role as plasticizer to increase ion dissociation as well as to remain the polymer electrolyte in a gel form by being trapped inside the polymer matrix. DMSO is commonly used as a solvent in professional field (Arya & Sharma, 2017; Singh *et al.*, 2012) because of its unique properties. The properties will play an important role when being apply in the DSSCs applications. According to reports,

DMSO has a low toxicity and a high dielectric constant of 47.24, thus high GPEs conductivity can be achieved due to the dissociation of salt into free ions has been ease (Aziz *et al.*, 2018).

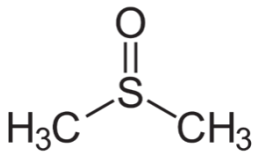

Figure 2.7. Chemical structure of DMSO

2.8 Lithium Iodide (LiI)

Lithium iodide (LiI) is a yellowish crystalline powder produced by the interaction of lithium hydride with iodine in diethyl ether. LiI is one of the iodide salt that was added to the electrolyte to improve ionic conductivity and PCE of DSSCs (Dissanayake *et al.*, 2014a; Noor *et al.*, 2014; Yusuf *et al.*, 2014). Iodide salt serves as a source of cations in the electrolyte as well as a supply of iodide/triiodide redox couples for the regeneration of oxidized dyes. As a result, it is necessary to examine the effects of iodide salts on electrolyte characteristics and DSSC performance (Ling *et al.*, 2020). According to Bandara *et al.* (2013), the size of the cation employed in the electrolytes affect the value of ionic conductivity and PCE of DSSCs (Bandara *et al.*, 2013). A small size and light weight of ion helps speed up the transport of the electrons from the counter electrode to the ionized dye. Hence, the PCE of the DSSCs increased. In this work, LiI play a role as an iodide supply in the GPEs to generate redox mechanisms for DSSCs. LiI will dissociate into free Li^+ and I^- ions (Figure 2.8) and assist to transfer electrons from the counter electrode to the ionized dyes by performing a redox process.

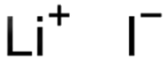

Figure 2.8. Chemical structure of Lithium Iodide

In order to re-generate the oxidized dye following the electron injection procedure, GPEs for DSSCs must additionally incorporate a redox mediator. Because of its high solubility, suitable redox potential, rapid dye renewal, and unfavorable electron recombination, the iodide/triiodide (I^-/I_3^-) redox pair is a desirable option (Arof *et al.*, 2018). Lithium iodide can provide high open circuit voltage in the solar cell so that the high efficiency of solar cell can be achieved because when there is high open circuit voltage, it will produce high efficiency (equation 3.10).

2.9 Iodine (I_2)

Iodine (I_2) is a chemical element with the atomic number of 53 and the symbol of I. Under normal condition, it exists as a semi-lustrous, non-metallic solid that melts to produce a deep violet liquid at 114°C and boils to form a violet gas at 114°C. In this work, I_2 is used to form iodide (I^-) or triiodide (I_3^-) redox mediator in the electrolyte which then plays an important role to transfer charge electrons from the counter electrode to the ionized dye in DSSCs. I^-/I_3^- redox mediator will provide high open circuit voltage (V_{oc}) in DSSCs because it has the ability to attract electron easily to form stable atom.

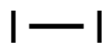

Figure 2.9. Chemical structure of Iodine

CHAPTER 3

METHODOLOGY

3.1 Introduction

This chapter explains the ways of the samples were prepared. Other than that, the set-up of the experiment and the characterizations exerted in conducting out this research project are also addressed. In this work, the liquid electrolyte system was first prepared to obtain the composition of highest conducting sample. The exact amount of dimethyl sulfoxide (DMSO) will be used and later will be stirred with different amount of lithium iodide (LiI) and iodide (I_2) salts to form liquid electrolytes. All the DMSO-LiI-I_2 liquid electrolytes prepared will be subjected to electrical impedance spectroscopy (EIS) to obtain the room temperature conductivity variations. A composition of DMSO-LiI-I_2 liquid electrolyte with the highest conductivity will then be added with varied amounts of gellan gum (GG) that acts as a host polymer in preparing gel polymer electrolytes (GPEs). All GPEs prepared will perform the impedance measurement using EIS. From the data, the charge carrier transport properties in each electrolyte were further evaluated. To test the potential of GG-DMSO-LiI-I_2 GPEs in DSSC applications, all GPEs prepared will be fabricated and exposed under 1000 W m^{-2} light illumination. The photovoltaic characteristics and EIS measurements will be performed on the fabricated cells to evaluate the power conversion efficiency of the DSSCs.

3.2 Sample Preparation

GG-based GPEs were prepared in this project. In this sample preparation, two systems have been constructed which are system 1 and system 2. System 1 preparing DMSO-LiI-I_2 liquid electrolytes. The room temperature conductivity of the liquid electrolyte in system 1 was initially determined. The electrolyte composition of highest room temperature conductivity in system 1 was then used as a reference to prepare GPEs of system 2. Different composition of GG that acts as a polymer host was added into the highest conducting electrolyte in DMSO-LiI-I_2 system to form GG-DMSO-LiI-I_2 gel polymer electrolytes.

3.2.1 DMSO-LiI-I_2 Liquid Electrolyte (System 1)

In system 1, DMSO-LiI-I_2 liquid electrolyte is prepared. The corresponding amount of LiI salt as shown in Table 3.1 is used to dissolve with 3.0000 g of DMSO in a closed bottle to form DMSO-LiI liquid electrolyte. The mixture is stirred and heated at 25°C for 30 minutes until a homogenous solution is obtained. Then, an appropriate amount of I_2 (refer Table 3.1) was added into the DMSO-LiI solution and stirred for 60 minutes at the same temperature. The homogenous liquid electrolytes were left to cool to room temperature (25°C) and stored overnight before being used for electrical impedance spectroscopy (EIS) characterization.

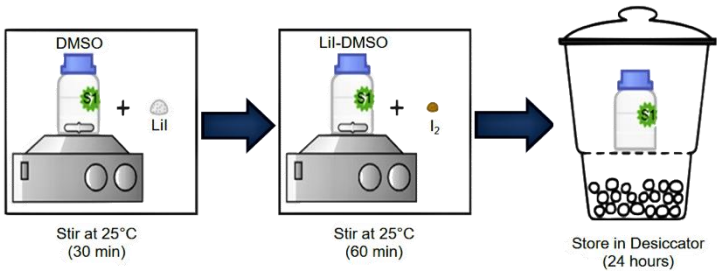

Figure 3.1. Preparation of DMSO-LiI-I_2 liquid electrolytes

Table 3.1. Composition of DMSO-LiI-I_2 liquid electrolytes

Designation	LiI (Molarity)	DMSO (g)	LiI (g)	I_2 (g)
LA1	0.6	3.0000	0.2190	0.0415
LA2	0.8	3.0000	0.2920	0.0554
LA3	1.0	3.0000	0.3650	0.0692
LA4	1.2	3.0000	0.4381	0.0831
LA5	1.4	3.0000	0.5111	0.0969

3.2.2 GG-DMSO-LiI-I_2 Gel Polymer Electrolyte (System 2)

The composition of highest room temperature conductivity electrolyte in system 1 chosen as a starting process in preparing GPEs of system 2. In this scenario, LA3 electrolyte with composition of 87.36 wt.% DMSO-10.62 wt.% LiI-2.02 wt.% I_2 was chosen since it revealed the highest conductivity of (10.77±0.38) mS cm^{-1} at room temperature. GG was added into the LA3 electrolyte in order to obtained gel-state polymer. The amount of 0.3650 g of LiI was dissolved into 3.0000 g of DMSO in a closed bottle and being stirred at 25°C for 30 minutes until a homogenous solution is obtained. Then, 0.0692 g of I_2 is added into the solution and continued to stir for the next 60 minutes at the same temperature. After that, the appropriate amount of GG as listed in Table 3.2 was added to the homogenous DMSO-LiI-I_2 electrolyte solution and stirred continuously at 70°C for 4 hours. The homogenous gel-like electrolytes were left to cool to room temperature and stored overnighter before being used for characterization.

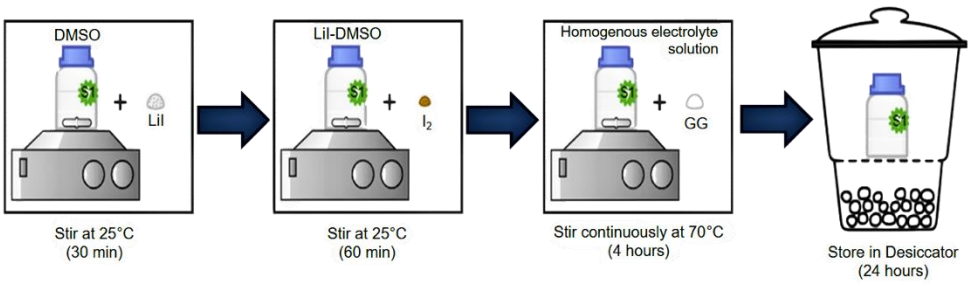

Figure 3.2. Preparation of GG-DMSO-LiI-I_2 gel polymer electrolytes

Table 3.2. Composition of GG-DMSO-LiI-I_2 gel polymer electrolytes

Designation	DMSO (g)	LiI (g)	I_2 (g)	GG (g)
GA1	3.0000	0.3650	0.0692	0.1500
GA2	3.0000	0.3650	0.0692	0.2000
GA3	3.0000	0.3650	0.0692	0.2500
GA4	3.0000	0.3650	0.0692	0.3000

3.3 Sample Characterization

3.3.1 Electrical Impedance Spectroscopy (EIS)

Electrical impedance spectroscopy (EIS) was carried out in order to identify the ion transport properties of prepared electrolytes. The electrolyte is filled in a coin cell and sandwiched between two stainless steel cell holder. The wire from the LCR meter (model HIOKI 3520 LCR Hi-Tester) was then be connected to both electrodes of the cell holder. This is because we want to get the even contact area and thickness (constant) and to use the closed system in order to minimize the moisture from outside air. After that, the electrolyte sample was being applied with 10 mV sinusoidal voltage. The impedance across the sample was measured between 50 Hz and 100 kHz at room (27°C) and elevated temperatures. From the data obtained, the complex impedance plot or known as Nyquist plot was constructed where a graph of negative imaginary impedance (Z'') against real impedance (Z') will be plotted. From the graph, the bulk resistance (R) of the electrolyte is determined from the intercept of the impedance plot with the horizontal axis as shown in Figure 3.3 (Noor, 2016).

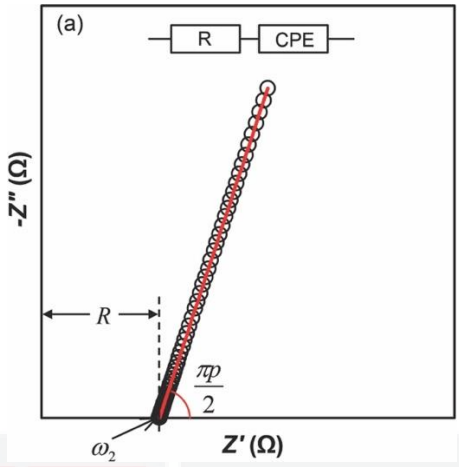

Figure 3.3. Nyquist plot consists of a tilted spike.

The ionic conductivity (σ) of the electrolyte was calculated using equation (3.1).

$$\sigma = \frac{t}{RA} \tag{3.1}$$

In the equation (3.1), t represents the thickness of electrolyte, A indicates the electrode/electrolyte contact area and R is the electrolyte bulk resistance.

3.3.2 Charge Carrier Transport Properties

In principle, the conductivity is related to the charge ion density (n), ion mobility (μ) and elementary charge (e) which is given in the equation (3.2).

$$\sigma = n\mu e \tag{3.2}$$

From equation (3.2), it shows that the charge carrier density and ion mobility are the crucial parameters that determined the electrolyte conductivity (Bandara *et al.*, 2017). Thus, these two parameters can be used quantitatively to examine the effect of salts as well as GG biopolymer in the electrolyte system on conductivity. Fitting the Nyquist plot with an appropriate derivate equivalent circuit equation can yield quantitative information on the diffusion coefficient (D), mobility (μ), and number density (n) of

charge carriers, as reported by Arof *et al.* (2017). Based on this work, the Nyquist plot presented a tilted spike. The optimum equations to match a tilted spike Nyquist plot, as shown in Figure 3.4 is the one derived from a circuit consisting of a resistor connected in series with a constant phase element (CPE). CPE is a non-ideal capacitor that models double-layer behaviour. The real (Z') and negative imaginary (Z'') impedance equations derived from the appropriate equivalent circuit are as below:

$$Z' = R + \frac{k\cos(\frac{\pi p}{2})}{\omega^p} \tag{3.3}$$

$$Z'' = \frac{k\sin(\frac{\pi p}{2})}{\omega^p} \tag{3.4}$$

In equations (3.3) and (3.4), R is the electrolyte bulk resistance, p is the slopping parameter that monitors the skewness of the tilted spike, and ω is the angular frequency (refer to Figure 3.4). The parameter k refers to the reciprocal of electrical double layer capacitance determined by trial and error until all the fitted points at the corresponding frequency matched with the experimental Nyquist plot. All parameter values obtained in the fitting method were then substituted in equations (3.5), (3.6) and (3.7) to estimate the D, μ and n of charge carrier in the electrolyte (Arof *et al.*, 2017).

$$D = D_0 \exp\left\{-0.158\left[\log_{10}(10)\right]^2 - 3.304\left[\log_{10}(10)\right] - 14.504\right\} \tag{3.5}$$

$$\mu = \frac{eD_0 \exp\left\{-0.158\left[\log_{10}(10)\right]^2 - 3.304\left[\log_{10}(10)\right] - 14.504\right\}}{k_b T} \tag{3.6}$$

$$n = \frac{\sigma k_b T}{e^2 D_0 \exp\left\{-0.158\left[\log_{10}(10)\right]^2 - 3.304\left[\log_{10}(10)\right] - 14.504\right\}} \tag{3.7}$$

where,

$$D_0 = \frac{4k^4 d^2}{R^4 \omega_2^3} \tag{3.8}$$

In equations (3.18) and (3.19), k_b is the Boltzmann constant, T is the absolute temperature and σ is the ionic conductivity (obtained from equation (3.1)). Parameter d refers to sample thickness, R is the electrolyte bulk resistance and ω_2 refers to the angular frequency at a minimum imaginary impedance ($-Z''$) (refer Figure 3.4).

3.4 Dye Sensitized Solar Cell (DSSC) Fabrication

3.4.1 TiO_2/Dye Electrode Preparation

Fluorine-doped tin oxide (FTO) glass has been used as a current collector in the preparation of titanium oxide (TiO_2) photoanode due to its good conductivity and transparency. The FTO glass was cleaned with detergent, rinsed with water and ethanol. The glass was then allowed to dry at ambient temperature. Two TiO2 layer was coated on the FTO glass. To prepare the first TiO_2 layer slurry, 0.5 g of P-90 TiO_2 powder was ground for 30 minutes in a mortar with 2 mL HNO_3 (pH = 1) before being spin-coated for 1 minute at 2350 rpm on a cleaned FTO glass to produce the compact layer. The FTO-glass coated substrate was then sintered for 45 minutes at 450°C before being allowed to cool at room temperature. The second TiO_2 layer was made by mixing and grinding 0.5 g of P-25 TiO_2 powder, 2 mL HNO_3 (pH = 1), 0.1 g carbowax, and 2 drops surfactant. The homogeneous paste was then drop on the first TiO_2 layer. Then, the doctor blade technique was performed to coat the porous layer (second layer) on the compact TiO_2 layer (first layer). The coated electrode was then sintered at 450°C before being allowed to cool to ambient temperature. The TiO_2 photoanode was then submerged in an ethanol solution containing 0.1 mM of N719 dye for 24 hours. The unbound TiO_2 particles and unabsorbed dye were removed by washing the

FTO/TiO_2/dye photoanode with ethanol before using it in DSSC fabrication and application.

3.4.2 Platinum (Pt) Counter Electrode Preparation

In this DSSCs application, the platinum (Pt) is chosen to be used as the counter electrode (CE). Because of its high conductivity and transparency, fluorine-doped tin oxide (FTO) glass has been utilized as a current collector. The FTO glass was cleansed with detergent and washed thoroughly with water and ethanol. The glass was then allowed to dry at ambient temperature. The FTO glass was placed on a hot plate and heated to 150°C. Plastisol (Solaronix), the commercial platinum solution was brushed over the FTO glass until the entire surface was coated. The electrode was then sintered for 45 minutes at 450°C before left to cool to room temperature.

3.4.3 Fabrication of Dye-Sensitized Solar Cells (DSSCs)

In order to test the potential of GG-DMSO-LiI-I_2 GPEs prepared, DSSCs was fabricated. The DSSCs was assembled by sandwiching the prepared GPEs between the dye/TiO_2 photoanode and Platinum (Pt) counter electrode in the configuration of FTO/TiO_2/N719 dye/GPE/Pt/FTO.

3.5 Characterization of Dye Sensitized Solar Cell (DSSC)

The fabricated DSSCs were exposed under a Xenon lamp with a 1000 Wm^{-2} light intensity. The Metrohm Autolab Potentiosat was then connected to the cell through the cable so that the photovoltaic (*J-V*) characteristics of the cell can be obtained. The DSSC had an exposed active area of 0.20 cm^2. A plot of current density

(*J*) against voltage (*V*) as in Figure 3.3 was then plotted from the obtained data. The fill factor (*FF*) was calculated using equation (3.9) (Devadiga *et al.*, 2021):

$$FF = \frac{J_{\max} \times V_{\max}}{J_{sc} \times V_{oc}} \tag{3.9}$$

Here, J_{max} and V_{max} is known as the maximum current density and the maximum voltage, respectively. J_{sc} and V_{oc} is respectively the current density at the short-circuit and open-circuit voltage. The power conversion efficiency (PCE) of DSSC was then be calculated using equation (3.10) (Devadiga *et al.*, 2021):

$$PCE(\%) = \frac{V_{oc} \times J_{sc} \times FF}{P_{in}} \times 100\% \tag{3.10}$$

In equation (3.10), P_{in} is known as incident light power density.

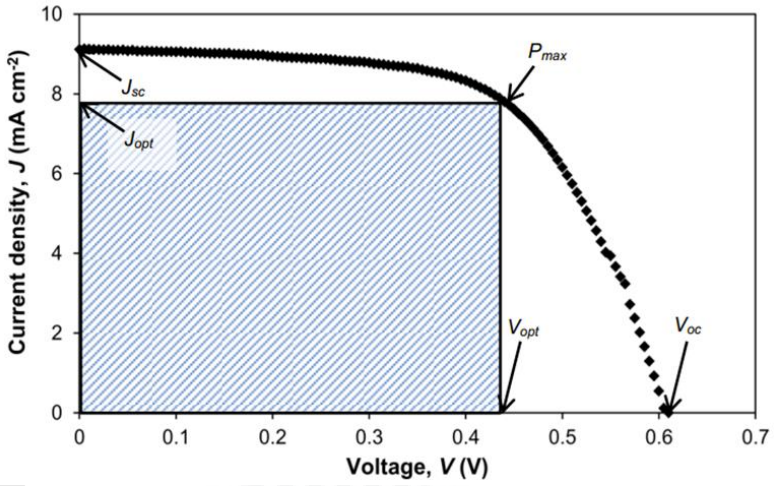

Figure 3.4. Photovoltaic measurement graph (Current density against voltage).

3.6 Electrochemical Impedance Characterizations of DSSC

The charge transfer resistance in DSSC can be determined by measuring the impedance of the DSSC. The impedance of DSSC has been performed using PGSTAT204 advanced electrochemical system (Metrohm Autolab) in the frequency range between 10 mHz and 1 MHz under 100 mW cm^{-2} light illumination at room temperature. The potential of each cell was set at their own V_{oc}.

CHAPTER 4

RESULTS AND DISCUSSION

4.1 Introduction

This chapter discuss about the results obtained from the characterization measurement. From electrical impedance spectroscopy (EIS), the dynamic ion properties in DMSO-LiI-I_2 liquid electrolytes (system 1) and GG-DMSO-LiI-I_2 gel polymer electrolytes (system 2) were evaluated at room and various temperature. The further explanations of the analysis for the charge transport properties of the prepared electrolytes also addressed. All the GG-DMSO-LiI-I_2 gel polymer electrolytes (GPEs) prepared have been fabricated into DSSCs in order to test its potential in the photovoltaic cells. The efficiency for all fabricated DSSCs were analyzed and explained.

4.2 DMSO-LiI-I_2 Liquid Electrolyte (System 1)

4.2.1 Electrical Impedance Spectroscopy (EIS) at Room Temperature

Figure 4.1 shows the Nyquist plots for DMSO-LiI-I_2 liquid electrolytes with different amount of LiI salt at room temperature (27°C). The plots show a titled spike shape indicating the high conducting nature of the electrolyte. The bulk resistance (R) value for each electrolyte was obtained from the intersection of plot with the horizontal axis. The conductivity of the electrolyte was calculated using the equation (3.1). The conductivity variation of electrolyte in system 1 is listed and presented in Table 4.1 and Figure 4.2, respectively.

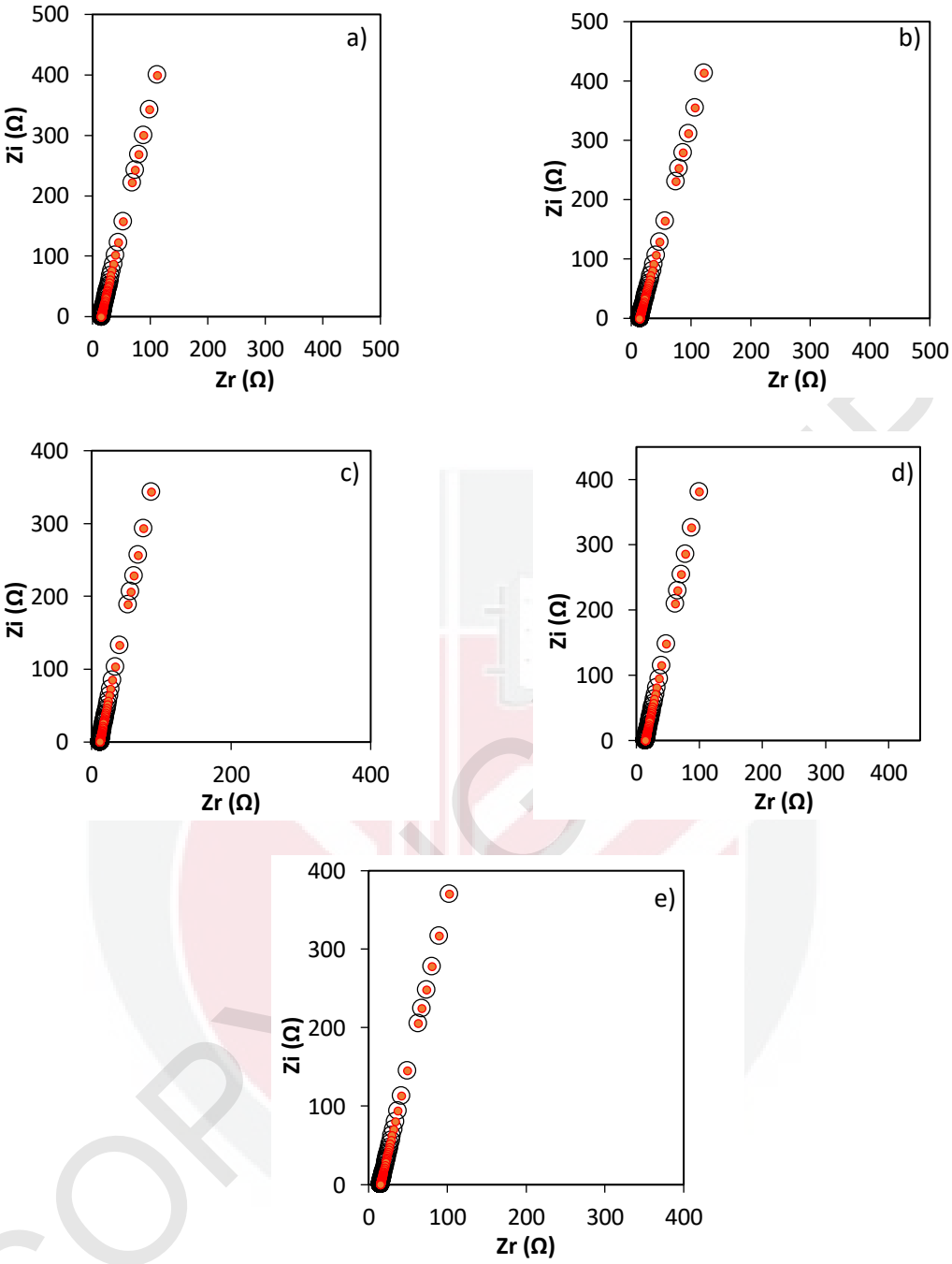

Figure 4.1. Nyquist plot with the corresponding fitted point for (a) LA1, (b) LA2, (c) LA3, (d) LA4 and (e) LA5 at room temperature.
(○ refer to experiment data and ● refer to fitted points)

Table 4.1. Room temperature conductivity, σ of DMSO-LiI-I_2 liquid electrolytes.

Electrolyte	σ (mS cm^{-1})
LA1	8.41±0.50
LA2	9.37±0.44
LA3	10.89±0.45
LA4	9.28±0.23
LA5	8.53±0.22

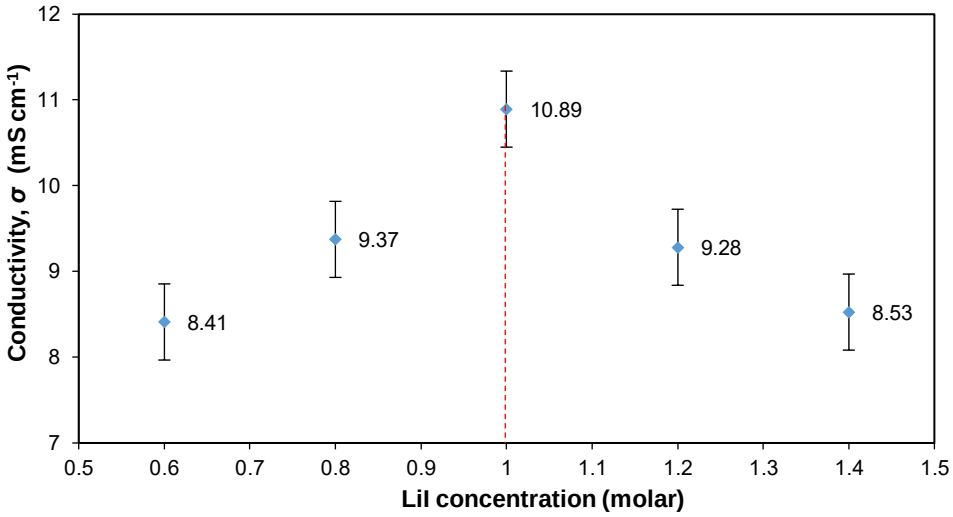

Figure 4.2. DMSO-LiI-I_2 liquid electrolytes system conductivity at room temperature.

From Table 4.1, it is clearly seen that electrolyte consists of 0.6 M LiI (LA1 electrolyte) has the conductivity value of (8.41±0.50) mS cm^{-1} at room temperature. The addition of LiI salt up to 0.8 M (LA2 electrolyte) is observed to increase the electrolyte conductivity to (9.37±0.44) mS cm^{-1} until it reaches the maximum conductivity value at room temperature of (10.89±0.45) mS cm^{-1} at 1.0 M of LiI (LA3 electrolyte). After that, the conductivity of the electrolyte is seen to slowly decrease to (9.28±0.23) mS cm^{-1} and (8.53±0.22) mS cm^{-1} at respectively 1.2 M of LiI (LA4 sample) and 1.4 M of LiI (LA5 sample). It is observed that the addition of LiI exceed the amount of salt in LA3 electrolyte has reduced the conductivity of the electrolyte. This is because the higher the amount of LiI increased the value of salt concentration which leads to the development of association ion. Thus, determination

of charge transport properties in DMSO-LiI-I_2 liquid electrolytes is performed to explain the conductivity behaviour in Figure 4.2. Hence, all the Nyquist plots obtained from EIS measurements in system 1 were fitted using equations (3.3) and (3.4).

4.2.2 Ionic Transport Properties at Room Temperature

The conductivity of electrolyte is affected by the mobility and the number density of the charge carrier. According to equation (3.2), the conductivity (σ) is the product of the charge carrier density (n) and the mobility (μ) with the elementary charge (e). Determine n and μ quantitatively explained the conductivity trend of electrolyte system. Charge transport properties can be evaluated by using fitting method. The experimental Nyquist plots in Figure 4.1 was fitted with equations (3.3) and (3.4). The obtained fitted parameters were substituted into equations (3.5), (3.6) and (3.7) to deduce respectively the values of diffusion coefficient (D), mobility (μ) and number density (n) of charge carrier. Figures 4.3, 4.4 and 4.5 represented the respective variations of the n, μ and D for DMSO-LiI-I_2 liquid electrolyte system at different LiI concentration.

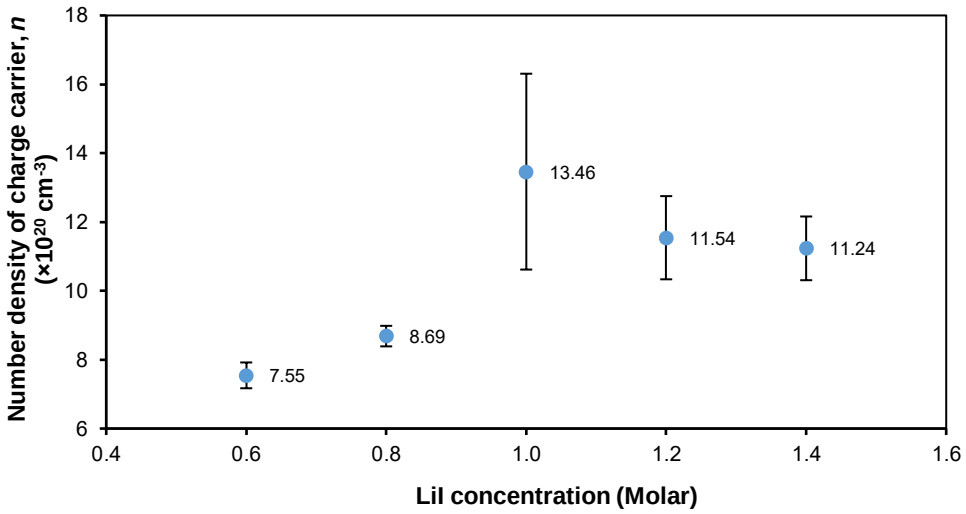

Figure 4.3. The number density of charge carrier, n for DMSO-LiI-I_2 liquid electrolyte sample at room temperature.

From Figure 4.3, the electrolyte of 0.6 M LiI in DMSO (LA1 electrolyte) produced free ion concentration of $(7.55\pm0.37)\times10^{20}$ cm^{-3}. The presence of the DMSO helps the salt to dissociate into free ions due to high dielectric constant of DMSO of ε_r = 47.24. DMSO was able the breakdown the lattice energy of LiI and dissociate the salt into Li^+ cations and I^- anions. As observed in Figure 4.3, the *n* increase in line with the increase of LiI salt concentration in DMSO. This circumstance occurred because the amount of dissociated salt increases as the LiI concentration continues to increase. The *n* keeps to increase gradually in electrolyte containing 0.8 M LiI (LA2 electrolyte) and 1.0 M LiI (LA3 electrolyte) with values of $(8.69\pm0.30)\times10^{20}$ cm^{-3} and $(13.46\pm2.84)\times10^{20}$ cm^{-3}, respectively. It can be seen that *n* shows a slight decrease to $(11.54\pm1.21)\times10^{20}$ cm^{-3} and $(11.24\pm0.93)\times10^{20}$ cm^{-3} as the amount of LiI in DMSO is respectively 1.2 M (LA4 electrolyte) and 1.4 M (LA5 electrolyte). This phenomenon can be attributed to an increase in ion association in the electrolyte. More free ions are dissociated when substantial amounts of salt are introduced into the polar aprotic solvent. In this situation, the free ions tend to be close to each other due to the restricted space between the ions in the solvent. When two opposing charges are relatively near each other, the greater attractive Coulomb force combine them thus form the ion association (Chowdhury *et al.*, 2020).

Figure 4.4 shows the variation of charge carrier mobility in DMSO-LiI-I_2 liquid electrolyte system at room temperature. LA1 electrolyte with 0.6 M of LiI in DMSO revealed the highest μ of $(6.96\pm0.25)\times10^{-5}$ cm^2 V^{-1} s^{-1} compared to other electrolytes. The μ is observed to decrease as the amount of LiI in the electrolyte increase. It is observed that μ has decrease in a large gap from $(6.75\pm0.45)\times10^{-5}$ cm^2 V^{-1} s^{-1} (μ of LA2 electrolyte) to $(5.18\pm1.17)\times10^{-5}$ cm^2 V^{-1} s^{-1} (LA3 electrolyte). The μ is then continued to decrease until obtained the lowest mobility of charge carrier of

$(4.77\pm0.47)\times10^{-5}$ cm^2 V^{-1} s^{-1} (LA5 electrolyte). The decrease in μ can be attributed to the amount of the charge carriers in the electrolytes being too dense to cause the ions to be difficult to move and collide with each other. As the concentration of LiI increases, the amount of charge carrier produced in the electrolytes also increases thus the tendency for ion collisions also increases results in a decrease in the mobility of the charge carriers in the liquid electrolyte.

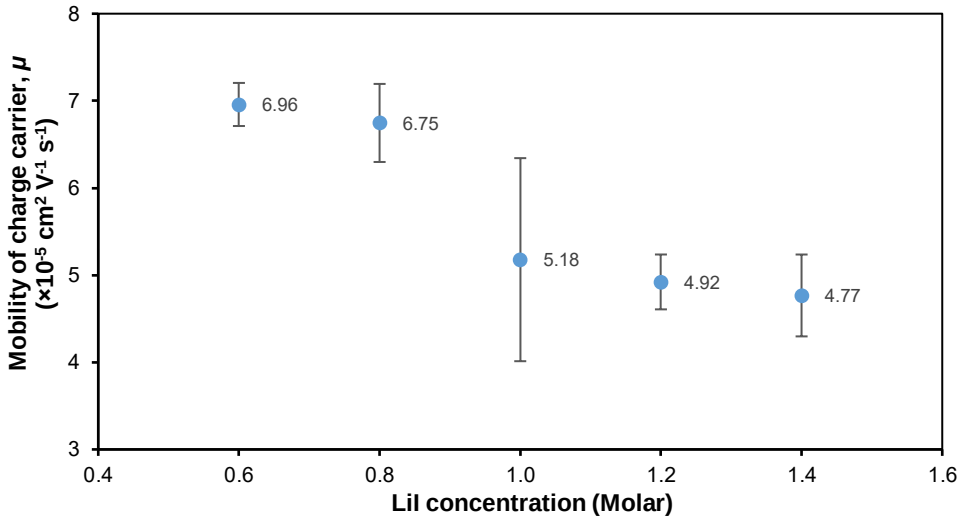

Figure 4.4. The mobility of charge carrier, μ for DMSO-LiI-I_2 liquid electrolyte sample at room temperature.

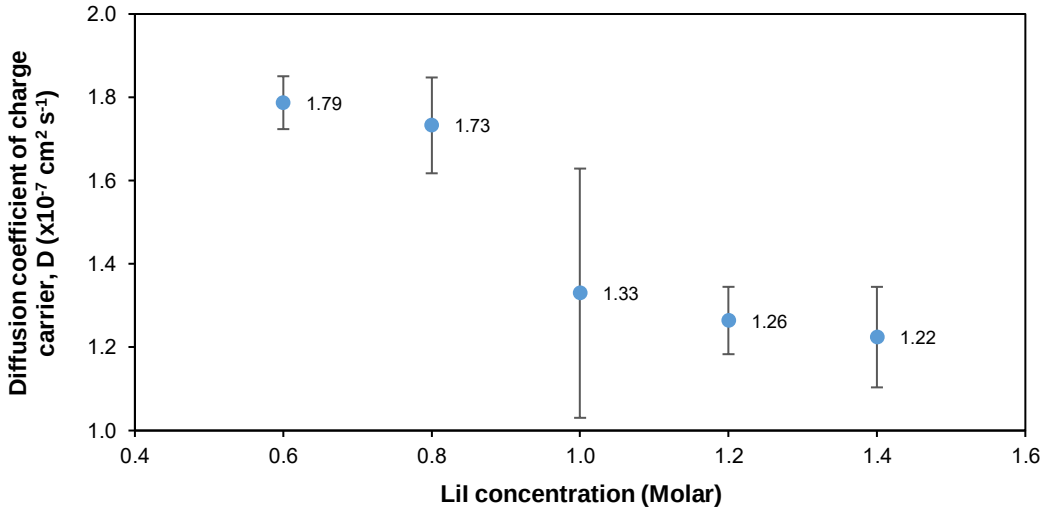

Figure 4.5. The diffusion coefficient of charge carrier, *D* for DMSO-LiI-I_2 liquid polymer electrolyte at room temperature.

The diffusion coefficient of charge carrier, D for DMSO-LiI-I_2 liquid polymer electrolyte at room temperature depicted in Figure 4.5 is seen to have a similar trend with μ for showed in Figure 4.4. The D is observed to slightly decrease from $(1.79\pm0.06)\times10^{-6}$ cm^2 s^{-1} (LA1 electrolyte) to $(1.73\pm0.12)\times10^{-6}$ cm^2 s^{-1} (LA2 electrolyte) and shows a tremendous gap to $(1.33\pm0.30)\times10^{-6}$ cm^2 s^{-1} (LA3 electrolyte). The D is seen to continued decrease slightly to $(1.26\pm0.08)\times10^{-6}$ cm^2 s^{-1} and $(1.2\pm0.12)\times10^{-6}$ cm^2 s^{-1} for LA3 and LA5 sample, respectively.

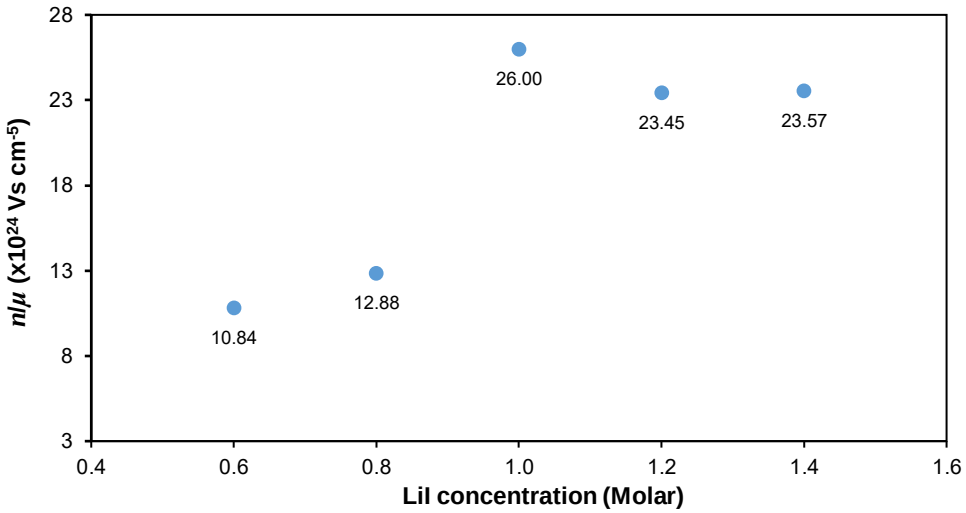

Figure 4.6. Variation of the ratio of n to μ for DMSO-LiI-I_2 liquid electrolyte system at room temperature.

Figure 4.6 depicts the variation of the ratio of n to μ for the DMSO-LiI-I_2 liquid electrolyte system. It is discovered that electrolyte containing of 1.0 M LiI (LA3 electrolyte) has a greatest ratio of $(26.00\pm2.44)\times10^{24}$ Vs cm^{-5}, indicating that the n contributes more to electrolyte conductivity than the μ. It can be concluded that the n is the most important component determining the conductivity of DMSO-LiI-I_2 liquid electrolytes obtained in Figure 4.2, rather than the μ and D.

4.3 GG-DMSO-LiI-I_2 Liquid Electrolyte (System 2)

The highest conductivity value obtained at room temperature for DMSO-LiI-I_2 liquid electrolyte (system 1) is (10.89 ± 0.45) mS cm^{-1} with the compositions of 87.36 wt.% DMSO-10.62 wt.% LiI-2.02 wt.% I_2 electrolyte (LA3 sample). This electrolyte composition was used as a starting composition in preparing the gellan gum (GG) based gel polymer electrolytes (GPEs) of system 2. Different amount of GG is added into LA3 electrolyte as shown in Table 3.2.

4.3.1 Electrical Impedance Spectroscopy (EIS) at Room Temperature

Electrical impedance spectroscopy (EIS) is a non-destructive approach, employed in this study to estimate the conductivity of the electrolyte. The dynamic ion characteristics in the prepared electrolyte was then being analyzed and discussed. Figure 4.7 shows the Nyquist plots for GG-LiI-I_2-DMSO GPEs with different GG composition measured at room temperature (27°C). All plots show only a titled spike shape. The bulk resistance value (*R*) is obtained from the intersection of plot with the horizontal axis and the conductivity of the electrolyte can be calculated using equation (3.1). The variation of room temperature conductivity of GPEs in system 2 is depicted in Figure 4.8.

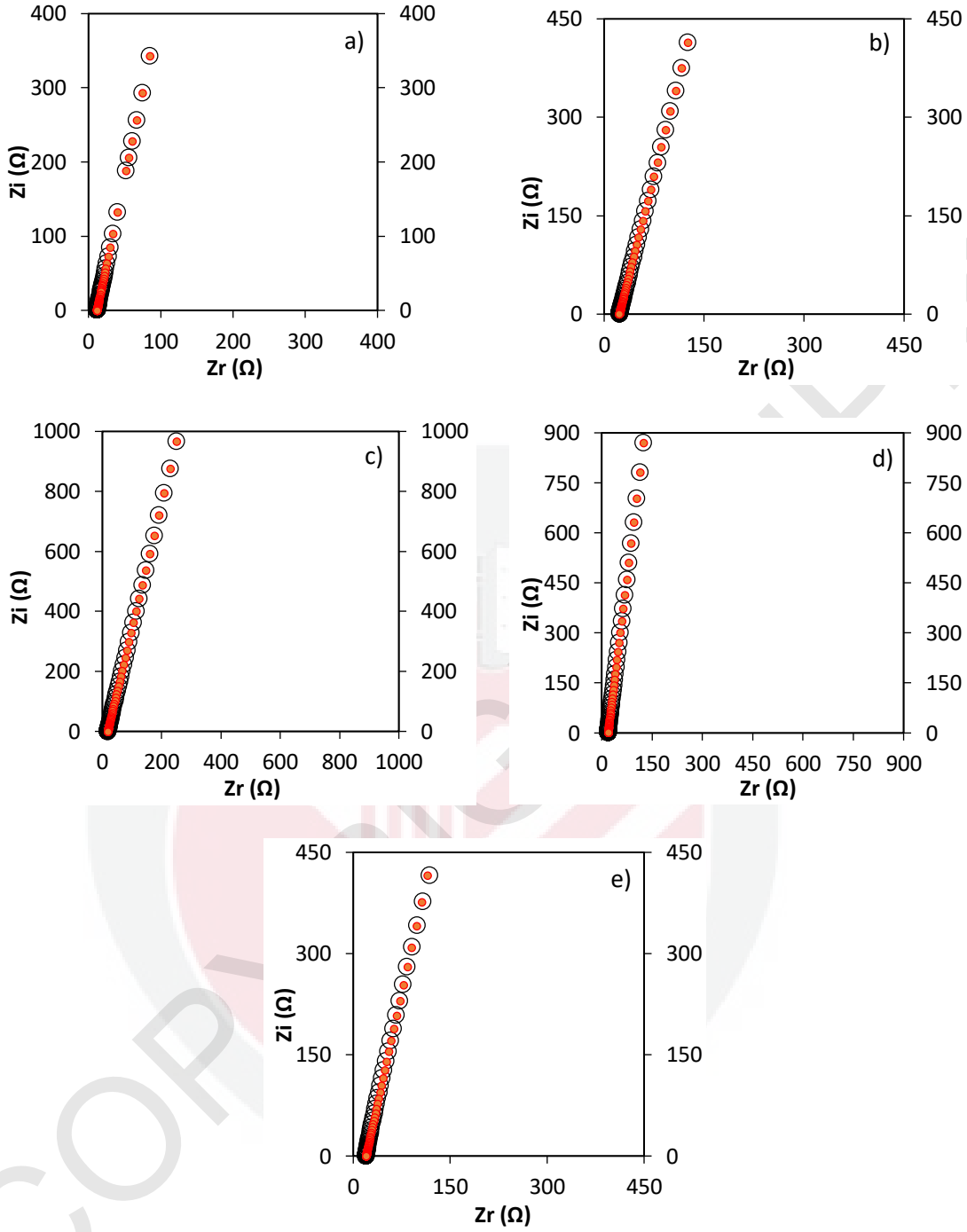

Figure 4.7. Nyquist plot with the corresponding fitted points for (a) LA3 (starting composition), (b) GA1, (c) GA2, (d) GA3 and (e) GA4 at room temperature. (○ refer to experimental data and ● refer to fitted points)

Table 4.2. Room temperature conductivity, σ of GG-DMSO-LiI-I_2 gel polymer electrolytes.

Electrolyte	σ (mS cm^{-1})
LA3	10.89
GA1	5.82
GA2	7.63
GA3	7.19
GA4	6.61

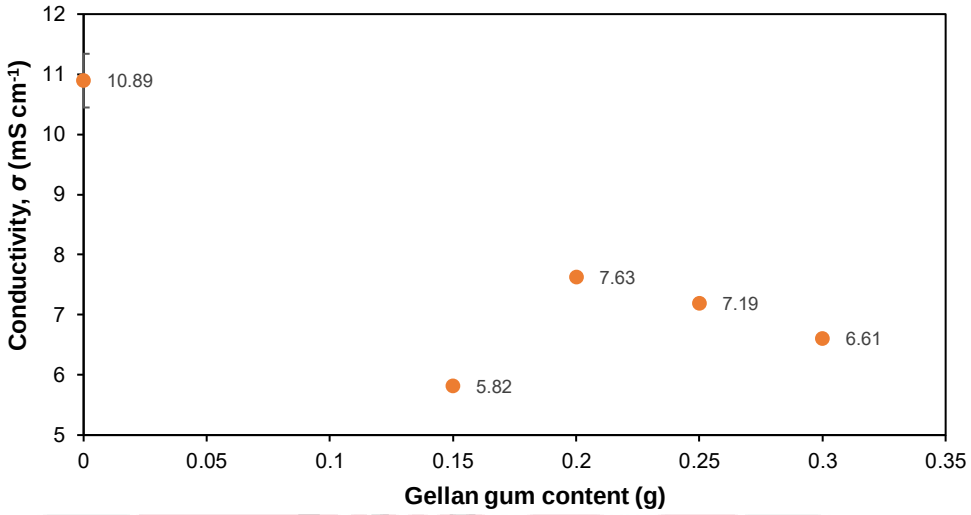

Figure 4.8. Variation of room temperature conductivity for GG-DMSO-LiI-I_2 gel polymer electrolyte systems.

From Table 4.2, the GG-free electrolyte (LA3 electrolyte) revealed the conductivity value of (10.89±0.45) mS cm^{-1} at room temperature. The addition of 0.15 g GG in LA3 electrolyte (now the GA1 electrolyte) is observed to decrease the conductivity to 5.82 mS cm^{-1} as shown in Figure 4.8. Further addition of GG in GA1 electrolyte is seen to increase the conductivity to 7.63 mS cm^{-1} with a GG content of 0.20 g. The conductivity is then observed to decrease when the amount of GG in LA3 electrolyte exceed 0.20 g. The addition of GG in LA3 electrolyte (the starting composition) is to produce GG-DMSO-LiI-I_2 GPE that changed the properties of the electrolyte sample from liquid to semi-solid state or known as gel state. As a result,

the conductivity of GPE is lower than that of liquid electrolyte because the movement of free ion as well as the concentration of free ions in the electrolyte is dropped. This is due to the limited space for ions to move as the amount of polymer added increases.

4.3.2 Ionic Transport Properties at Room Temperature

To investigate the conductivity trend obtained in Figure 4.8, all the Nyquist plots in Figure 4.7 was fitted with equations (3.3) and (3.4). All parameter values acquired are then entered into equations (3.5), (3.6), and (3.7) to compute the n, μ and D of the charge carriers in the GG-DMSO-LiI-I_2 electrolytes.

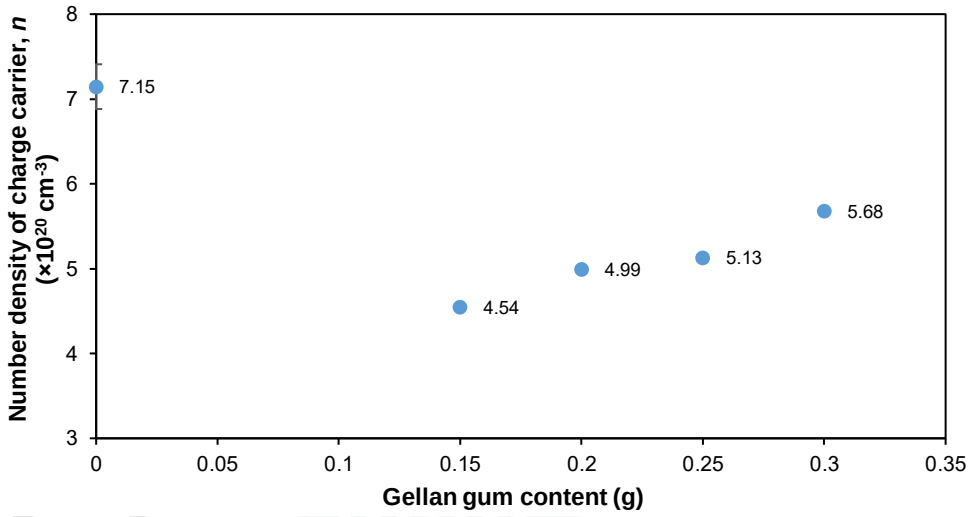

Figure 4.9. The number density of charge carrier, n for GG-DMSO-LiI-I_2 gel polymer electrolyte system at room temperature.

Figure 4.9 shows the trend of n in GG-DMSO-LiI-I_2 GPEs at room temperature. It can be seen that LA3 electrolyte (GG-free electrolyte) has the n of $(7.15\pm2.64)\times10^{20}$ cm^{-3}. The n is then dropped to 4.54×10^{20} cm^{-3} after 0.15 g GG was introduced. The n is then continuing to increase as the amount of GG increased up to a maximum of 5.68×10^{20} cm^{-3} with electrolyte consisting of 0.30 g GG (GA4 electrolyte). The reason

of this happens because the ionic bond that attract LiI in the electrolyte are broken. When more GG is added into the DMSO-LiI-I_2 liquid electrolyte, GG delivered surplus electrons to facilitate the dissociation of the LiI salt, resulting in an increase in *n* in the electrolyte.

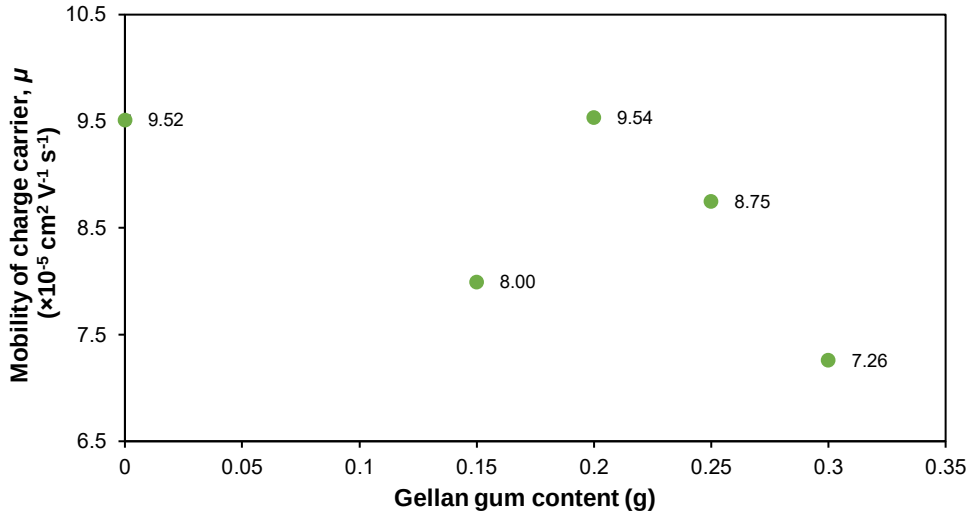

Figure 4.10. The mobility of charge carrier, μ for GG-DMSO-LiI-I_2 gel polymer electrolyte system at room temperature.

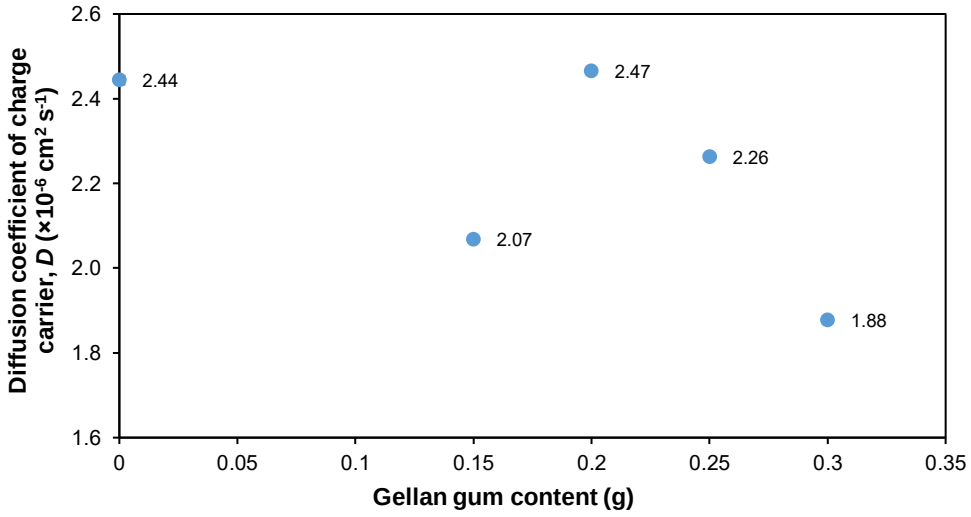

Figure 4.11. Diffusion coefficient of charge carrier, *D* for GG-DMSO-LiI-I_2 gel polymer electrolyte system at room temperature.

Figures 4.10 and 4.11 indicate identical findings of trend in the mobility (μ) and diffusion coefficient (D) of charge carriers as a function of GG concentration. The μ and D are observed to reduce respectively to 8.00×10^{-5} cm^2 V^{-1} s^{-1} and 2.07×10^{-6} cm^2 s^{-1} as 0.15 g GG was added into LA3 electrolyte. The μ and D are shown to increase to 9.54×10^{-5} cm^2 V^{-1} s^{-1} and 2.47×10^{-6} cm^2, respectively when 0.20 g of GG (LA2 electrolyte) was added, but then drop after several GG was further added in LA2 electrolyte. As explained previously, when the amount of GG added is more than 0.15 g, n in GPE is increased. It caused a limited space for the free ions to move around randomly in the electrolyte medium (Chowdhury *et al.*, 2020). As a result, more collision will occur between them and thus reduce μ and D.

4.3.3 Conductivity at Various Temperature

Figure 4.12 shows the conductivity-temperature variation of GG-DMSO-LiI-I_2 GPEs. From Figure 4.12, it can be seen that the conductivity of all electrolytes increases with increasing temperature from 27°C (room temperature) to 100°C. As observed in Figure 4.12, GA2 and GA3 electrolytes has achieved a conductivity value that overlapped with each other at 40°C and 45°C. Besides, at temperature of 50°C, GA2 sample is again overlapped with the other GA4 electrolyte. This phenomenon occurred because of the conductivity value at the specific temperature between the two electrolytes are too close which are 10.48 mS cm^{-1} and 10.44 mS cm^{-1} at 40°C for GA2 and GA3 electrolytes respectively although the concentration of GG in both samples are different. Similar trend occurred at 45°C, where the GA2 and GA3 electrolytes achieved the respectively conductivity of 11.79 mS cm^{-1} and 11.80 mS cm^{-1}. This overlapped plots also happens between GA2 and GA4 electrolytes.

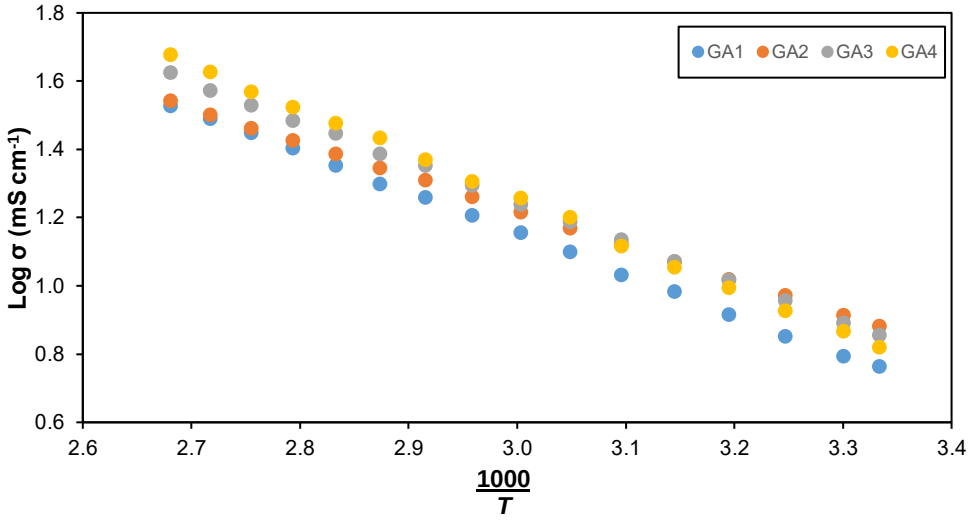

Figure 4.12. Conductivity at varied temperature of GG-DMSO-LiI-I_2 gel polymer electrolyte system.

4.3.4 Ionic Transport Properties at Various Temperature

All the Nyquist data obtained at various temperature were fitted with equations (3.3) and (3.4). All parameter values acquired are then entered into equations (3.5), (3.6), and (3.7) to deduce the n, μ and D of the charge carriers in the GG-DMSO-LiI-I_2 electrolytes at various temperature.

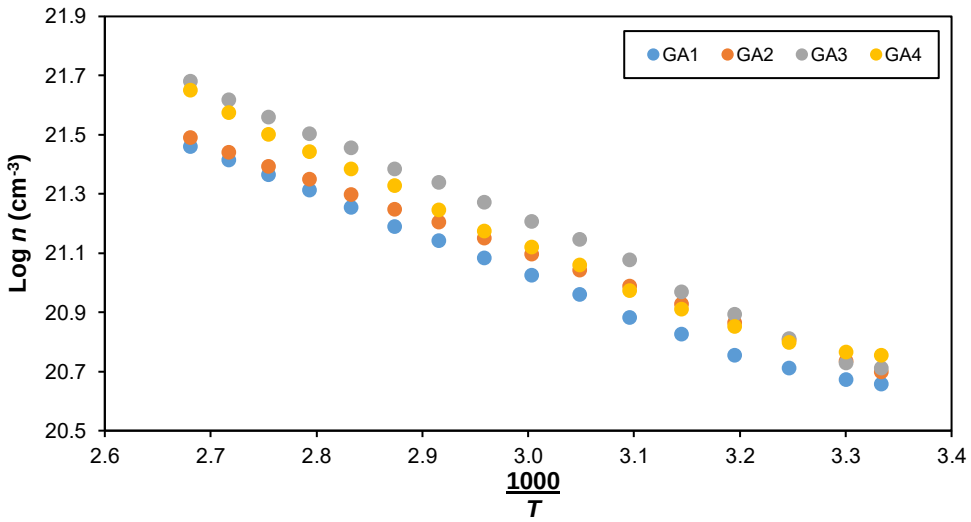

Figure 4.13. The charge carrier number density, n for GG-DMSO-LiI-I_2 gel polymer electrolyte system at varied temperatures.

Figure 4.13 depicts a trend of *n* at different temperature. It can be seen that *n* increases with temperature. As the temperature rose, so did the heat energy, allowing more ions in the electrolyte to dissociate. This is because more heat energy was absorbed by the LiI, cause each atom to vibrate at a high frequency. The binding energy between Li^+ and I^- was then became weak, thus contributed to ion dissociation. As a result, the ion concentration increased as the temperature increased (Tan *et al.*, 2019).

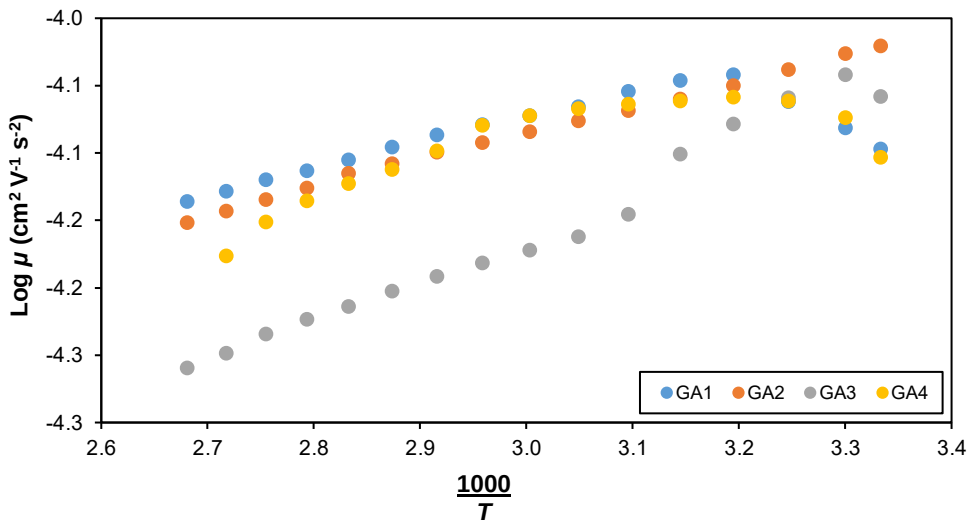

Figure 4.14. The mobility of charge carrier, μ for GG-DMSO-LiI-I_2 gel polymer electrolyte system at various temperatures.

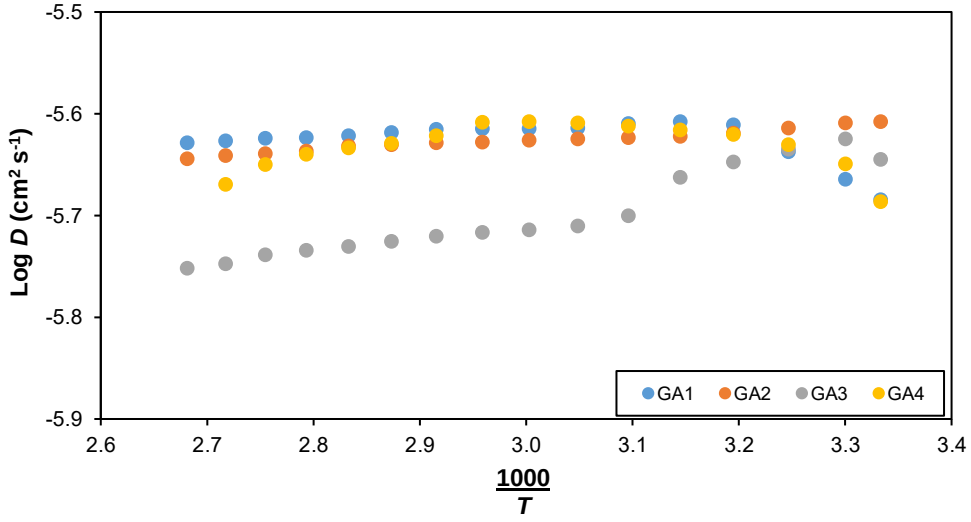

Figure 4.15. The diffusion coefficient of charge carrier, *D* for GG-DMSO-LiI-I_2 gel polymer electrolyte system at various temperatures.

Figures 4.14 and 4.15 shows the variation of μ and D for GG-DMSO-LiI-I_2 GPE system at various temperatures. Referring to Figures 4.14 and 4.15, the μ and D increase from 27°C to 40°C before it continues to decrease except for GA2 sample in which μ and D is keep decreasing from room temperature until 100°C. The decrement plots happen when the n increases as observed from Figure 4.13, causing the ions and the GG polymer matrix to draw closer together. As a result, when an electric field is applied, the ions move randomly in the confined region, and ion collisions occur, causing the μ and n to diminish (Chowdhury *et al.*, 2020).

4.4 Photovoltaic Performance of DSSC with GG-DMSO-LiI-I_2 Gel Polymer Electrolytes

All GPEs prepared in this work have been used as charge transfer medium in dye sensitized solar cells (DSSCs). The photovoltaic characteristics of the DSSCs fabricated with these samples are depicted in Figure 4.16. From Figure 4.16, the parameters of short-circuit current density (J_{sc}), open-circuit voltage (V_{oc}), fill factor (FF) and power conversion efficiency (PCE) were obtained and listed in Table 4.3.

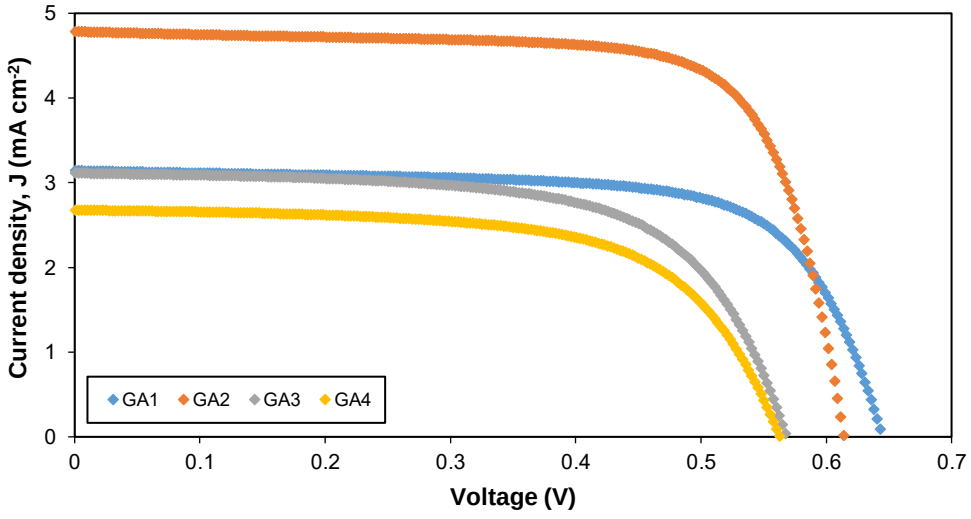

Figure 4.16. Photovoltaic characteristics of DSSCs with GG-DMSO-LiI-I_2 GPEs

Table 4.3. Values of J_{sc}, V_{oc}, *FF* and PCE for DSSC fabricated with GG-DMSO-LiI-I_2 GPEs

Sample	J_{sc} (mA cm^{-2})	V_{oc} (V)	*FF* (%)	PCE (%)
GA1	3.083 ± 0.031	0.642 ± 0.001	0.706 ± 0.003	1.397 ± 0.013
GA2	4.787 ± 0.004	0.612 ± 0.002	0.736 ± 0.002	2.154 ± 0.013
GA3	3.097 ± 0.014	0.571 ± 0.002	0.642 ± 0.001	1.134 ± 0.003
GA4	2.673 ± 0.005	0.564 ± 0.002	0.636 ± 0.002	0.959 ± 0.001

During the photovoltaic process, the TiO_2 conduction band of the DSSC is shifted to the negative potential under visible light illumination of 100 mW cm^{-2}. The difference in potential between the TiO_2 Fermi level (energy level towards the bottom of the TiO_2 conduction band) and the electrolyte's redox potential is defined as the open-circuit voltage (V_{oc}). When an electrolyte is sandwiched between the TiO_2/dye photoanode and counter electrode, the free cations from the electrolyte are absorbed and aggregated on the mesoporous TiO_2 (Cahen *et al.*, 2000; Chowdhury *et al.*, 2020; Watson & Meyer, 2004). As a result of this process, the TiO_2 conduction band becomes a little positive, and the TiO_2 conduction band and Fermi level are carried towards the valence band (Cahen *et al.*, 2000; Chowdhury *et al.*, 2020; Watson & Meyer, 2004). As the number of free ions in the sandwiched GPE increases, more free cations will be adsorbed and generated on the surface of TiO_2 mesoporous. Because of the highly positive condition of the TiO_2 conduction band, the conduction band and Fermi level of TiO_2 shift away to the positive potential (i.e. valence band). As a result, the open-circuit voltage (V_{oc}) of the cell will decrease.

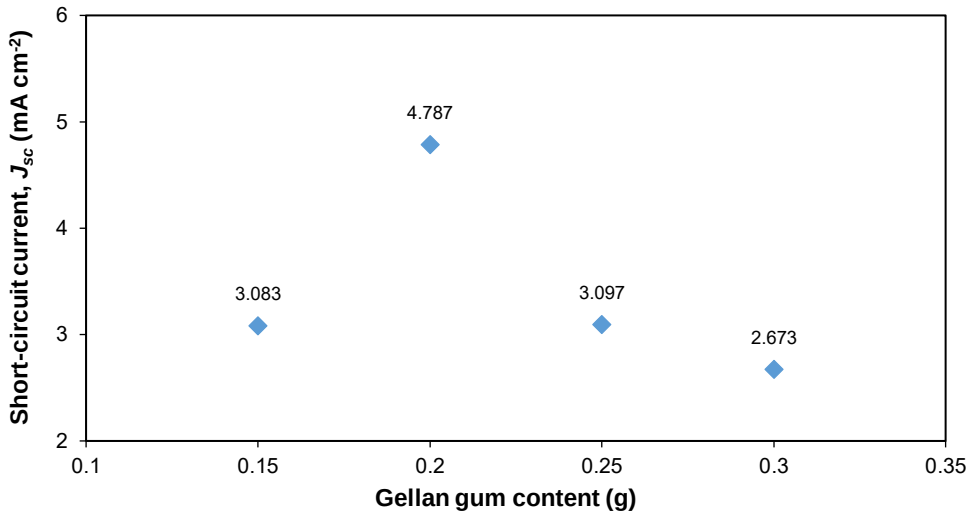

Figure 4.17. Variation of short-circuit current, J_{sc} of DSSCs fabricated with GG-DMSO-LiI-I_2 gel polymer electrolyte systems.

J_{sc} denotes the charge transport conductivity from the excited state of the dye to the conduction band of the metal oxide, as well as the charge transport conductivity from the counter electrode to the ionized dye (Aziz *et al.*, 2021; Chowdhury *et al.*, 2020). In another word, J_{sc} is the current flow through the solar cell when there is no voltage across the solar cell (means when the solar cell is short circuited). Based on Figure 4.17, the value of J_{sc} is seen to increase from (3.08±0.03) mA cm^{-2} for DSSC with GA1 electrolyte to (4.79±0.01) mA cm^{-2} for DSSC with GA2 electrolyte, which the highest J_{sc} value obtained in this work. The increase in J_{sc} may be influence by the increase in n, μ and D observed in Figures 4.9, 4.10 and 4.11. The J_{sc} is seen to decrease to (3.10±0.01) mA cm^{-2} for DSSC with GA3 electrolyte and reach the lowest J_{sc} value of (2.673±0.005) mA cm^{-2} for DSSC with GA4 electrolyte. As seen in Figures 4.10 and 4.11, the decrement value can be attributed to the decrease in μ and D that reduce the transfer of electron from the counter electrode to the ionized dye, in turn lower the J_{sc} value of DSSCs (Aziz *et al.*, 2021).

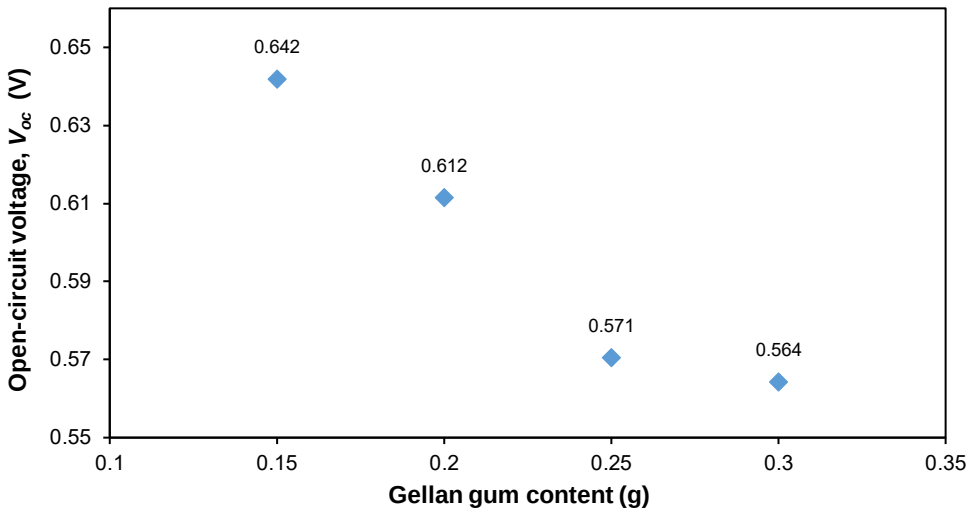

Figure 4.18. Variation of the open-circuit voltage, V_{oc} of DSSCs fabricated with GG-DMSO-LiI-I_2 gel polymer electrolyte systems.

As refer to Figure 4.18, the variation of the open-circuit voltage (V_{oc}) of DSSCs fabricated with GG-DMSO-LiI-I_2 GPEs have a decrement trend. DSSC with GA1 electrolyte has the highest V_{oc} of (0.64±0.01) V before it started to decrease as the GG content in the sample increases. The lowest achieved V_{oc} in this project is (0.56±0.02) V for the DSSC with GA4 electrolyte. It can be seen that the presence of GG in the electrolyte sample has reduce the V_{oc} value. This is in line with the increased in n observed from Figure 4.9, which has lowered the TiO_2 conduction band as well as TiO_2 Fermi level towards the valence band and thus smaller the energy gap between the TiO_2 Fermi level and the redox potential. As a results, the V_{oc} decreased.

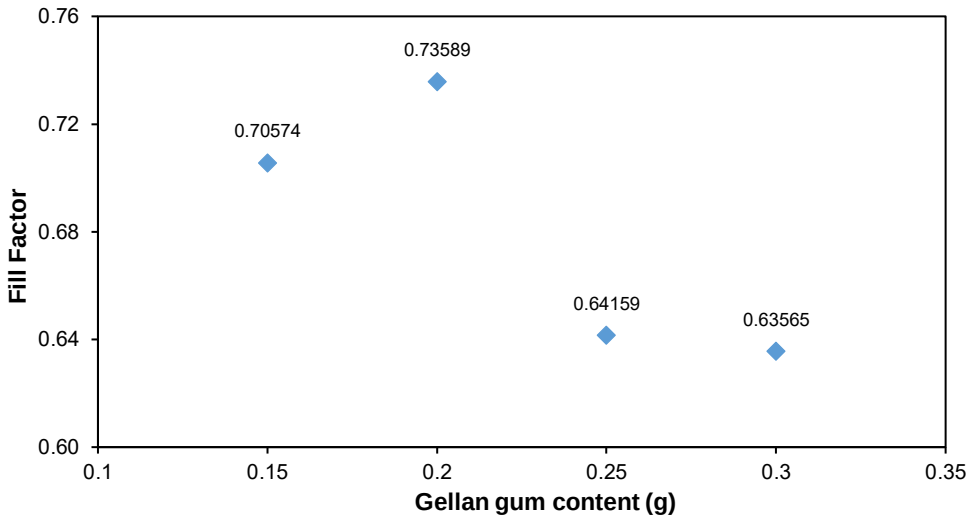

Figure 4.19. Variation of the fill factor of DSSCs fabricated with GG-DMSO-LiI-I_2 gel polymer electrolyte systems.

Based on Table 4.3, the fill factor value for all DSSCs are between 63% and 74%. This clearly proven that the GPEs had an excellent contact between the counter electrode and the photoanode, yielding a good charge transfer (Aziz *et al.*, 2021). The DSSC fabricated with GA2 electrolyte had achieved the highest power conversion efficiency (PCE) of (2.154±0.013) %. The highest J_{sc} in DSSC fabricated with GA2 electrolyte is due to the highest conductivity value achieved by GA2 electrolyte, which is driven by the highest μ and n. These parameters have promoted the electron shift from the counter electrode to the ionized dye, resulting in the greatest PCE of DSSC. As a result, it is important to emphasize that the addition of GG into the LA3 electrolyte in order to produce a GPE system positively affected the PCE of DSSCs.

4.5 Electrochemical Impedance Spectroscopy for DSSCs with GG-DMSO-LiI-I_2 Gel Polymer Electrolytes

Impedance for DSSC was performed with the purpose to reinforce the findings obtained in Chapter 4.4. In order to evaluate the resistance at each interaction of a

DSSC, EIS was performed on the DSSC. The EIS for DSSC comprises the three depressed semicircles as shown in Figure 4.20 (Chowdhury *et al.*, 2020). The charge transfer resistance (R_{pt}) at the electrolyte/counter electrode interface is represented by the first depressed semicircle in the high frequency region. The resistance of charge transfer (R_{ct}) at the TiO_2/dye/electrolyte interface is indicated by the second depressed semicircle in the middle frequency range. The electron diffusion resistance (R_d) of the redox electrolyte is referred to the final depressed semicircle in the low frequency zone.

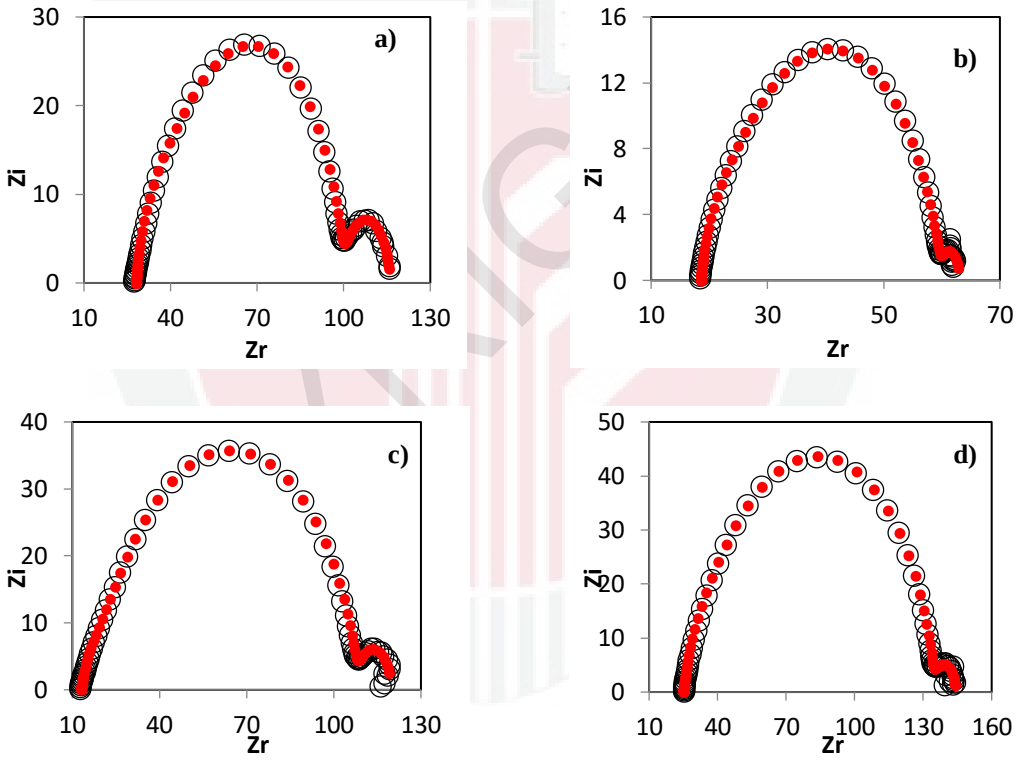

Figure 4.20. Nyquist plot and their corresponding fitted point for (a) GA1, (b) GA2, (c) GA3, and (d) GA4 DSSCs of GG-DMSO-LiI-I_2 gel polymer electrolytes. (○ refer to experiment data and ● refer to fitted points)

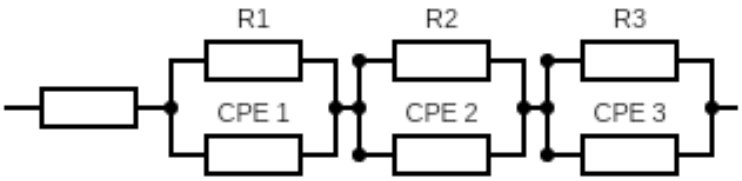

Figure 4.21. The diagrams of the equivalent circuit representing to the EIS plot for DSSCs. R1=R_{pt}, R2=R_{ct}, R3=R_d, respectively.

Based on Figure 4.20, the resistance between the origin and interception of an impedance plot at high frequency corresponding to the FTO substrate's serial resistance (R_s). Other than that, R_{ct} is particularly crucial in this study since it is related to J_{sc} obtained from the photovoltaic measurement. Thus, the impedance data in Figure 4.20 was fitted with the equivalent circuit corresponding to a resistor in series with three parallel circuits comprising a resistor in parallel with a constant phase element, as illustrated in Figure 4.21. The derivative equation is as below:

$$Z' = R_s + \left[\sum_{i=1}^{3} \frac{R_i + R_i^2 k_i^{-1} \omega^{p_i} \cos\left(\frac{\pi p_i}{2}\right)}{1 + 2R_i k_i^{-1} \omega^{p_i} \cos\left(\frac{\pi p_i}{2}\right) + R_i^2 k_i^{-2} \omega^{2p_i}} \right] \tag{4.8}$$

$$Z'' = \sum_{i=1}^{3} \frac{R_i^2 k_i^{-1} \omega^{p_i} \sin\left(\frac{\pi p_i}{2}\right)}{1 + 2R_i k_i^{-1} \omega^{p_i} \cos\left(\frac{\pi p_i}{2}\right) + R_i^2 k_i^{-2} \omega^{2p_i}} \tag{4.9}$$

Based on equations (4.8) and (4.9), R is the resistance at the respective electrode interfaces. Figure 4.20 shows the Nyquist plot with the corresponding fitted point (● refer to fitted points) for a DSSC fabricated with GG-DMSO-LiI-I_2 GPEs. Table 4.4 shows the R_{ct} value obtained from the fitting method.

Table 4.4. Value of charge transfer resistance (R_{ct}) of DSSCs fabricated with GG-based GPEs obtained from Figure 4.16

Electrolyte	R_{ct} (Ω)
GA1	59.0
GA2	36.5
GA3	85.5
GA4	98.5

Based on data tabulated in Table 4.4, the R_{ct} for DSSC with GA1 electrolyte is 59.0 Ω. When 0.20 g of GG was added to LA3 electrolyte, the R_{ct} reduced to 36.5 Ω. As seen in Figures 4.9 and 4.10, decreases in R_{ct} can be associated to an increase in n and μ. The drop in R_{ct} improves electron charge transport from the dye excited state to the TiO_2 conduction band, resulting in a high J_{sc}. Referring to Table 4.3, DSSC with GA2 electrolyte had the highest J_{sc} value of (4.79±0.01) mA cm^{-2}, proving that the charge transfer resistance is reduced in DSSCs fabricated with GA2 electrolyte composition. The R_{ct} rise up to 85.5 Ω when the DSSC was fabricated with GA3 electrolyte. The J_{sc} appears to decrease to (3.10±0.01) mA cm^{-2}, meaning that electron charge transport is slowing down. As seen in Figures 4.10 and 4.11, this occurrence can be attributed to a reduction in μ and D. As a conclusion, the inverted trend found for R_{ct} when compared to the trend for J_{sc} demonstrated that DSSC was improved owing to the concentration of free charge carriers and its mobility.

CHAPTER 5

CONCLUSIONS

In this work, gellan gum (GG) based gel polymer electrolytes (GPEs) consisting of different composition of lithium iodide (LiI) salt and Iodine (I_2) were successfully obtained. The production of this GPEs has achieved one of the main objectives of this project.

One of the aims for this research was to evaluate the charge transport properties in GG-DMSO-LiI-I_2 GPEs at room and various temperature. The study of electrical impedance spectroscopy for the system 1 shows that the DMSO-LiI-I_2 liquid electrolyte with 1 M of LiI (LA3 electrolyte) revealed the highest room temperature conductivity value of (10.89±0.45) mS cm^{-1} compared to other liquid electrolytes prepared. The highest conductivity value in LA3 electrolyte was influence by the highest of charge carrier concentration (n), not its mobility (μ). LA3 electrolyte was then being used as starting composition to produce the GPEs of system 2. The conductivity of was slightly decrease to 5.82 mS cm^{-1} when 0.15 g GG (GA1 electrolyte) was added due to the increase in n and μ. The conductivity was then increase to 7.63 mS cm^{-1} as 0.20 g of GG is added into LA3 electrolyte (now GA2 electrolyte). The conductivity was then observed to decrease as more GG was added. The conductivity trend in GG-DMSO-LiI-I_2 GPEs was mainly govern by μ, not n. The conductivity-temperature studies show that the conductivity increase with increasing temperature. The n in the electrolyte had the greatest impact on the trend of conductivity at various temperatures in all GPEs prepared.

The next objective of this study was to test the potential of GG-DMSO-LiI-I_2 GPEs in dye sensitized solar cells (DSSCs). All prepared GPEs were used as a redox

medium in DSSCs. The study shows that DSSC fabricated with GA2 electrolyte had the best power conversion efficiency (PCE) value of (2.15±0.01) % compared to the other fabricated cells. The highest short-circuit current density (J_{sc}) of DSSC computed was (4.787±0.004) mA cm^{-2}, which is affected by the great μ and n in GA2 electrolyte. It is proved by the EIS measurement showed the DSSC fabricated with GA2 electrolyte has the lowest charge transfer resistance (R_{ct}). The average fill factor of 68% for all developed DSSC demonstrates that GPEs have excellent contact with the counter electrode and photoanode, which improves the electron transfer mechanism.

According to the findings of this research, the produced GPEs are seen to have a high potential as a medium for charge transfer in DSSCs. This is due to the high conductivity of ~10^{-3} S cm^{-1} as well as the outstanding charge carrier transport capabilities of this electrolyte, which makes it a strong candidate for usage in DSSCs. This study yielded a few ideas for future research, which are listed below:

- Adding additive (plasticizer, ionic liquid and/or salt) into the GPEs to increase the conductivity.
- Adding 4-tert-butylpyridine (TBP) or guanidinium thiocyanate (GuSCN) to increase V_{oc} of DSSC
- Study the electron dynamic (recombination and transfer of charge) using intensity-modulated photocurrent/photovoltage spectroscopy (IMPS/IMVS)

REFERENCES

A. K., Amirudin, S., Yusof, S. Z., & Noor, I. M. (2014). A method based on impedance spectroscopy to determine transport properties of polymer electrolytes. Physical Chemistry Chemical Physics, 16(5), 1856–1867. https://doi.org/10.1039/c3cp53830c

Abdukarimov, A., Shah, S., & Buraidah, L. P. T. M. H. (2020). Characteristics of dye - sensitized solar cells (DSSCs) using liquid and gel polymer electrolytes with tetrapropylammonium salt. Optical and Quantum Electronics, 52(3), 1–15. https://doi.org/10.1007/s11082-020-02264-1

Abdukarimov, A. A., Ikramov, R. G., Mamatkarimov, O. O., & Arof, A. K. (2020). Dependence of the characteristics of dye-sensitized solar cells on amount tetrapropylammonium iodide. 22(4), 250–253.

Aram, E., Ehsani, M., & Khonakdar, H. A. (2015). Improvement of ionic conductivity and performance of quasi-solid-state dye sensitized solar cell using PEO/PMMA gel electrolyte. Thermochimica Acta, 615, 61–67. https://doi.org/10.1016/j.tca.2015.07.006

Arof, A. K., Aziz, M. F., Noor, M. M., Careem, M. A., Bandara, L. R. A. K., Thotawatthage, C. A., Rupasinghe, W. N. S., & Dissanayake, M. A. K. L. (2014). Efficiency enhancement by mixed cation effect in dye-sensitized solar cells with a PVDF based gel polymer electrolyte. International Journal of Hydrogen Energy, 39(6), 2929–2935. https://doi.org/10.1016/j.ijhydene.2013.07.028

Arof, A. K., Mat Nor, N. A., Ramli, N. R., Aziz, N., Noor, I. M., & Taha, R. M. (2017). Utilization of saffron (Crocus sativus L.) as sensitizer in dye-sensitized solar cells (DSSCs). *Optical and Quantum Electronics*, *49*(1), 11082. https://doi.org/10.1007/s11082-016-0882-6

Arof, A. K., Noor, I. M., Buraidah, M. H., Bandara, T. M. W. J., Careem, M. A., Albinsson, I., & Mellander, B. E. (2017). Polyacrylonitrile gel polymer electrolyte based dye sensitized solar cells for a prototype solar panel. Electrochimica Acta, 251, 223–234. https://doi.org/10.1016/j.electacta.2017.08.129

Arya, A., & Sharma, A. L. (2017). Polymer electrolytes for lithium ion batteries: a critical study. In *Ionics* (Vol. 23, Issue 3). Ionics. https://doi.org/10.1007/s11581-016-1908-6

Aziz, M. F., Noor, M. A. A. I. M., & Arof, M. H. B. A. K. (2021). Impact of Diethyl carbonate in PVA based gel polymer electrolytes on dye - sensitized solar cells performance. *Optical and Quantum Electronics*, *53*(1), 1–16. https://doi.org/10.1007/s11082-020-02724-8

Azmi, M. I., Mansor, Y., Tamchek, N., & Noor, I. M. (2021). Influence of Ion Transport Parameters on Conductivity at Room Temperature in DMSO-TPAI-I_2 Electrolyte. 9(December), 56–61.

Bandara, T. M. W. J., Fernando, H. D. N. S., Furlani, M., Albinsson, I., Dissanayake, M. A. K. L., Ratnasekera, J. L., & Mellander, B. E. (2017). Dependence of solar cell performance on the nature of alkaline counterion in gel polymer electrolytes containing binary iodides. *Journal of Solid State Electrochemistry*, *21*(6), 1571–1578. https://doi.org/10.1007/s10008-017-3518-2

Bandara, T. M. W. J., Jayasundara, W. J. M. J. S. R., Dissanayake, M. A. K. L., Furlani, M., Albinsson, I., & Mellander, B.-E. (2013). Effect of cation size on the performance of dye sensitized nanocrystalline tio2 solar cells based on quasi-solid state pan electrolytes containing quaternary ammonium iodides. Electrochimica Acta, 109, 609–616. https://doi.org/10.1016/j.electacta.2013.07.089

Bandara, T. M. W. J., Karunathilaka, D. G. N., Ratnasekera, J. L., & De, L. A. (2017). *Electrical and complex dielectric behaviour of composite polymer electrolyte based on PEO, alumina and tetrapropylammonium iodide*. 1711–1719. https://doi.org/10.1007/s11581-017-2016-y

Bharadwaz, A., & Jayasuriya, A. C. (2020). Materials Science & Engineering C Recent trends in the application of widely used natural and synthetic polymer nanocomposites in bone tissue regeneration. *Materials Science & Engineering C*, *110*(January), 110698. https://doi.org/10.1016/j.msec.2020.110698

Buraidah, M. H., Shah, S., Teo, L. P., Chowdhury, F. I., Careem, M. A., Albinsson, I., Mellander, B. E., & Arof, A. K. (2017). High efficient dye sensitized solar cells using phthaloylchitosan based gel polymer electrolytes. *Electrochimica Acta*, *245*, 846–853. https://doi.org/10.1016/j.electacta.2017.06.011

Buraidah, M., Shah, S., Teo, L., Chowdhury, F. I., Careem, M., Albinsson, I., Mellander, B. E., & Arof, A. (2017). High efficient dye sensitized solar cells using phthaloylchitosan based gel polymer electrolytes. Electrochimica Acta, 245, 846–853. https://doi.org/10.1016/j.electacta.2017.06.011

Cahen, D., Hodes, G., Grätzel, M., Guillemoles, J. F., & Riess, I. (2000). Nature of photovoltaic action in dye-sensitized solar cells. The Journal of Physical Chemistry B, 104(9), 2053–2059. https://doi.org/10.1021/jp993187t

Careem, M. A., Aziz, M. F., & Buraidah, M. H. (2017). Boosting Efficiencies of Gel Polymer Electrolyte Based Dye Sensitized Solar Cells Using Mixed Cations. Materials Today: Proceedings, 4(4), 5092–5099. https://doi.org/10.1016/j.matpr.2017.05.013

Chai, K. L., Noor, I. M., Aung, M. M., Abdullah, L. C., & Kufian, M. Z. (2020). Non-edible oil based polyurethane acrylate with tetrabutylammonium iodide gel polymer electrolytes for dye-sensitized solar cells. *Solar Energy*, *208*(July), 457–468. https://doi.org/10.1016/j.solener.2020.08.020

Chen, J., Peng, T., Shi, W., Li, R., & Xia, J. (2013). An efficient binary ionic liquid based quasi solid-state electrolyte for dye-sensitized solar cells. Electrochimica Acta, 107, 231–237. https://doi.org/10.1016/j.electacta.2013.06.014

Chen, K.-F., Liu, C.-H., Hsieh, C.-K., Lin, C.-L., Huang, H.-K., Tsai, C.-H., & Chen, F.-R. (2014). New fabrication process of long-life dye-sensitized solar cells by in situ gelation of quasi-solid polymer electrolytes. Journal of Power Sources, 247, 939–946. https://doi.org/10.1016/j.jpowsour.2013.08.103

Chowdhury, F. I., Buraidah, M. H., Arof, A. K., Mellander, B. E., & Noor, I. M. (2020). Impact of tetrabutylammonium, iodide and triiodide ions conductivity in polyacrylonitrile based electrolyte on DSSC performance. *Solar Energy*, *196*(December 2019), 379–388. https://doi.org/10.1016/j.solener.2019.12.033

Čolović, M., Volavšek, J., Stathatos, E., Čelan Korošin, N., Šobak, M., & Jerman, I. (2019). Amphiphilic POSS-based ionic liquid electrolyte additives as a boost for dye-sensitized solar cell performance. *Solar Energy*, *183*(February), 619–631. https://doi.org/10.1016/j.solener.2019.03.070

Devadiga, D., Selvakumar, M., Shetty, P., & Santosh, M. S. (2021). Recent progress in dye sensitized solar cell materials and photo-supercapacitors: A review. Journal of Power Sources, 493(February). https://doi.org/10.1016/j.jpowsour.2021.229698

Edman, L., Doeff, M. M., Ferry, A., Kerr, J., & De Jonghe, L. C. (2000). Transport properties of the solid polymer electrolyte system P(EO)NLITFSI. The Journal of Physical Chemistry B, 104(15), 3476–3480. https://doi.org/10.1021/jp993897z

Farhana, N. K., Ramesh, S., & Ramesh, K. (2019). Efficiency enhancement of dye-sensitized solar cell based gel polymer electrolytes using Poly (vinyl butyral-co-vinyl alcohol-co-vinyl acetate)/tetrapropylammonium iodide. *Materials Science in Semiconductor Processing*, *91*(November 2018), 414–421. https://doi.org/10.1016/j.mssp.2018.12.007

Greek, A., & War, S. W. (2018). *Introduction to Plastics Engineering*. 1–16. https://doi.org/10.1016/B978-0-323-39500-7.00001-0

He, J., Duffy, N. W., Pringle, J. M., & Cheng, Y.-B. (2013). Conducting polymer and titanium carbide-based nanocomposites as efficient counter electrodes for dye-sensitized solar cells. Electrochimica Acta, 105, 275–281. https://doi.org/10.1016/j.electacta.2013.05.005

Jun, T., Kim, K., Lee, K. M., Murale, D. P., Singh, A. P., Natsagdorj, A., Liew, H., Suh, Y.-H., & Churchill, D. G. (2012). The inorganic DMSO/pocl3 reaction with Bodipy: Wide product formation and implications for Biological Ros Sensing and Neurodegenerative Disease Research. Journal of Porphyrins and Phthalocyanines, 16(11), 1201–1208. https://doi.org/10.1142/s1088424612501180

Kakati, B. K., Sathiyamoorthy, D., Verma, A. (2010). Electrochemical and mechanical behavior of carbon composite bipolar plate for fuel cell. International Journal of Hydrogen Energy, 35(9), 4185–4194. https://doi.org/10.1016/j.ijhydene.2010.02.033

Kakiage, K., Aoyama, Y., Yano, T., Oya, K., Fujisawa, J. I., & Hanaya, M. (2015). Highly-efficient dye-sensitized solar cells with collaborative sensitization by silyl-anchor and carboxy-anchor dyes. *Chemical Communications*, *51*(88), 15894–15897. https://doi.org/10.1039/c5cc06759f

Köhnen, E., Wagner, P., Lang, F., Cruz, A., Li, B., Roß, M., Jošt, M., Morales-Vilches, A. B., Topič, M., Stolterfoht, M., Neher, D., Korte, L., Rech, B., Schlatmann, R., Stannowski, B., & Albrecht, S. (2021). 27.9% Efficient Monolithic Perovskite/Silicon Tandem Solar Cells on Industry Compatible Bottom Cells. *Solar RRL*, *2100244*, 1–8. https://doi.org/10.1002/solr.202100244

Li, Q., Chen, X., Tang, Q., Cai, H., Qin, Y., He, B., Li, M., Jin, S., & Liu, Z. (2014). Enhanced photovoltaic performances of quasi-solid-state dye-sensitized solar cells using a novel conducting gel electrolyte. Journal of Power Sources, 248, 923–930. https://doi.org/10.1016/j.jpowsour.2013.10.025

Ling, C. K., Aung, M. M., Abdullah, L. C., Hong Ngee, L., & Uyama, H. (2020). A short review of iodide salt usage and properties in dye sensitized solar cell application: Single vs binary salt system. Solar Energy, 206(April), 1033–1038. https://doi.org/10.1016/j.solener.2020.06.055

Liu, S., Chen, X., & Zhang, Y. (2020). Hydrogels and hydrogel composites for 3D and 4D printing applications. 3D and 4D Printing of Polymer Nanocomposite Materials, 427–465. doi:10.1016/b978-0-12-816805-9.00014-4

Mohamad Sri, M. N. S., Buraidah, M. H., & Teo, L. P. (2017). Effect of 1-butyl-3-methylimidazolium iodide on the performance of dye-sensitized solar cell having PEO-PVA based gel polymer electrolyte. Materials Today: Proceedings, 4(4), 5161–5168. https://doi.org/10.1016/j.matpr.2017.05.022

Mohamad, A. A. (2019). Physical properties of quasi-solid-state polymer electrolytes for dye-sensitised solar cells: A characterisation review. Solar Energy, 190(August), 434–452. https://doi.org/10.1016/j.solener.2019.08.016

Mohapatra, S. R., Thakur, A. K., & Choudhary, R. N. P. (2009). Effect of nanoscopic confinement on improvement in ion conduction and stability properties of an intercalated polymer nanocomposite electrolyte for energy storage applications. Journal of Power Sources, 191(2), 601–613. https://doi.org/10.1016/j.jpowsour.2009.01.100

Moore, K., & Wei, W. (2021). Applications of carbon nanomaterials in perovskite solar cells for solar energy conversion. Nano Materials Science, March. https://doi.org/10.1016/j.nanoms.2021.03.005

Mulmi, S., Park, C. H., Kim, H. K., Lee, C. H., Park, H. B., & Lee, Y. M. (2009). Surfactant-assisted polymer electrolyte nanocomposite membranes for fuel cells. Journal of Membrane Science, 344(1-2), 288–296. https://doi.org/10.1016/j.memsci.2009.08.028

Neto, M. J., Sentanin, F., Esperança, J. M. S. S., Medeiros, M. J., Pawlicka, A., De Zea Bermudez, V., & Silva, M. M. (2015). Gellan gum - Ionic liquid membranes for electrochromic device application. *Solid State Ionics*, *274*, 64–70. https://doi.org/10.1016/j.ssi.2015.02.011

Noor, I. M. (2020). Determination of charge carrier transport properties of gellan gum–lithium triflate solid polymer electrolyte from vibrational spectroscopy. High Performance Polymers, 32(2), 168–174. https://doi.org/10.1177/0954008319890016

Noor, I. S. M., Majid, S. R., Arof, A. K., Djurado, D., Claro Neto, S., & Pawlicka, A. (2012). Characteristics of gellan gum-LiCF3SO3polymer electrolytes. Solid State Ionics, 225, 649–653. https://doi.org/10.1016/j.ssi.2012.03.019

Noor, I. S., Majid, S. R., & Arof, A. K. (2013). Poly (vinyl alcohol)-LiBOB complexes for lithium-air cells. Electrochimica Acta, 102, 149–160. https://doi.org/10.1016/j.electacta.2013.04.010

Noor, M. M., Aziz, M. F., Arof, A. K., Careem, M. A., Bandara, L. R. A. K., Thotawatthage, C. A., Rupasinghe, W. N. S., Dissanayake, M. A. K. L. (2014). Efficiency enhancement by mixed cation effect in dye-sensitized solar cells with a PVDF based gel polymer electrolyte. International Journal of Hydrogen Energy, 39(6), 2929–2935. https://doi.org/10.1016/j.ijhydene.2013.07.028

Praveen, E., Peter, I. J., Kumar, A. M., Ramachandran, K., & Jayakumar, K. (2020). Boosting of Power Conversion Efficiency of 2D ZnO Nanostructures-Based DSSC by the Lorentz Force with Chitosan Polymer Electrolyte. *Journal of Inorganic and Organometallic Polymers and Materials*, *30*(12), 4927–4943. https://doi.org/10.1007/s10904-020-01629-z

Reinsberg, P., Abd-El-Latif, A.-E.-A. A., & Baltruschat, H. (2018). Investigation of the complex influence of divalent cations on the oxygen reduction reaction in aprotic solvents. Electrochimica Acta, 273, 424–431. https://doi.org/10.1016/j.electacta.2018.03.123

Rivas, B. L., & Maureira, A. (2008). Water-soluble polyelectrolytes contaning sulfonic acid groups with metal ion binding ability by using the liquid phase polymer based retention technique. Macromolecular Symposia, 270(1), 143–152. https://doi.org/10.1002/masy.200851017

Rudhziah, S. (2022). Hybrid carboxymethyl kappa-carrageenan/carboxymethyl cellulose- based biopolymer electrolytes for dye-sensitized solar cell application. International Journal of Electrochemical Science, 17, ArticleID:220143. https://doi.org/10.20964/2022.01.41

Rudra, S., Woo, H., Sarker, S., & Min, D. (2021). Journal of Industrial and Engineering Chemistry Simulation and electrochemical impedance spectroscopy of dye-sensitized solar cells. Journal of Industrial and Engineering Chemistry, 97, 574–583. https://doi.org/10.1016/j.jiec.2021.03.010

Samarasingha, P. B., Wijayasinghe, A., Behm, M., Dissanayake, L., & Lindbergh, G. (2014). Development of cathode materials for lithium ion rechargeable batteries based on the system Li(Ni1/3MN1/3Co(1/3-X)MX)O2, (M=mg, Fe, Al and X=0.00 to 0.33). Solid State Ionics, 268, 226–230. https://doi.org/10.1016/j.ssi.2014.07.012

Selvanathan, V., Yahya, R., Alharbi, H. F., Alharthi, N. H., Alharthi, Y. S., Ruslan, M. H., Amin, N., & Akhtaruzzaman, M. (2020). Organosoluble starch derivative as quasi-solid electrolytes in DSSC: Unravelling the synergy between electrolyte rheology and photovoltaic properties. *Solar Energy*, *197*(December 2019), 144–153. https://doi.org/10.1016/j.solener.2019.12.074

Shah, S., Noor, I. M., Pitawala, J., Albinson, I., Bandara, T. M., Mellander, B.-E., & Arof, A. K. (2017). Plasmonic effects of quantum size metal nanoparticles on dye-sensitized solar cell. Optical Materials Express, 7(6), 2069. https://doi.org/10.1364/ome.7.002069

Singh, R., Bhattacharya, B., Rhee, H. W., & Singh, P. K. (2015). Solid gellan gum polymer electrolyte for energy application. *International Journal of Hydrogen Energy*, *40*(30), 9365–9372. https://doi.org/10.1016/j.ijhydene.2015.05.084

Singh, R., Jadhav, N. A., Majumder, S., Bhattacharya, B., & Singh, P. K. (2013). Novel biopolymer gel electrolyte for dye-sensitized solar cell application. *Carbohydrate Polymers*, *91*(2), 682–685. https://doi.org/10.1016/j.carbpol.2012.08.055

Su'ait, M. S., Rahman, M. Y. A., & Ahmad, A. (2015). Review on polymer electrolyte in dye-sensitized solar cells (DSSCs). Solar Energy, 115, 452–470. https://doi.org/10.1016/j.solener.2015.02.043

Suhaimi, S., Shahimin, M. M., Alahmed, Z. A., Chyský, J., & Reshak, A. H. (2015). Materials for enhanced dye-sensitized solar cell performance: Electrochemical application. International Journal of Electrochemical Science, 10(4), 2859–2871.

Suresh Kumar, N., & Chandra Babu Naidu, K. (2021). A review on perovskite solar cells (pscs), materials and applications. Journal of Materiomics, 7(5), 940–956. https://doi.org/10.1016/j.jmat.2021.04.002

Tan, H. W., Ramesh, S., & Liew, C. (2019). *Electrical, thermal, and structural studies on highly conducting additive-free biopolymer electrolytes for electric double-layer capacitor application*. 4861–4874.

Teo, L. P., Tiong, T. S., Buraidah, M. H., & Arof, A. K. (2018). Effect of lithium iodide on the performance of dye sensitized solar cells (DSSC) using poly (ethylene oxide) (PEO)/poly (vinyl alcohol) (PVA) based gel polymer electrolytes. *Optical Materials*, *85*(May), 531–537. https://doi.org/10.1016/j.optmat.2018.09.026

Upadhyaya, H. M., Senthilarasu, S., Hsu, M.-H., & Kumar, D. K. (2013). Recent progress and the status of dye-sensitised solar cell (DSSC) technology with state-of-the-art conversion efficiencies. Solar Energy Materials and Solar Cells, 119, 291–295. https://doi.org/10.1016/j.solmat.2013.08.031

Venkatesan, S., Hidayati, N., Liu, I.-P., & Lee, Y.-L. (2016). Highly efficient gel-state dye-sensitized solar cells prepared using propionitrile and poly (vinylidene fluoride-co-hexafluoropropylene). Journal of Power Sources, 336, 385–390. https://doi.org/10.1016/j.jpowsour.2016.11.014

Venkatesan, S., Liu, I. P., Hung, W. N., Teng, H., & Lee, Y. L. (2019). Highly efficient quasi-solid-state dye-sensitized solar cells prepared by printable electrolytes for room light applications. *Chemical Engineering Journal*, *367*(1), 17–24. https://doi.org/10.1016/j.cej.2019.02.118

Verma, D., Katti, K. S., & Katti, D. R. (2010). Osteoblast adhesion, proliferation and growth on polyelectrolyte complex–hydroxyapatite nanocomposites. Philosophical Transactions of the Royal Society A: Mathematical, Physical and Engineering Sciences, 368(1917), 2083–2097. https://doi.org/10.1098/rsta.2010.0013

Wanninayake, W. M. N. M. B., Premaratne, K., Kumara, G. R. A., & Rajapakse, R. M. G. (2016). Use of lithium iodide and tetrapropylammonium iodide in gel electrolytes for improved performance of quasi-solid-state dye-sensitized solar cells: Recording an efficiency of 6.40%. Electrochimica Acta, 191, 1037–1043. https://doi.org/10.1016/j.electacta.2016.01.108

Watson, D. F., & Meyer, G. J. (2004). Cation effects in nanocrystalline solar cells. Coordination Chemistry Reviews, 248(13-14), 1391–1406. https://doi.org/10.1016/j.ccr.2004.02.015

Yuan, S., Tang, Q., He, B., & Zhao, Y. (2014). Multifunctional graphene incorporated conducting gel electrolytes in enhancing photovoltaic performances of quasi-solid-state dye-sensitized solar cells. Journal of Power Sources, 260, 225–232. https://doi.org/10.1016/j.jpowsour.2014.03.034

Yun, S., Hagfeldt, A., & Ma, T. (2014). Pt-free counter electrode for dye-sensitized solar cells with high efficiency. *Advanced Materials (Deerfield Beach, Fla.)*, *26*(36), 6210–6237. https://doi.org/10.1002/adma.201402056

Yusuf, S. N. F., Aziz, M. F., Hassan, H. C., Bandara, T. M. W. J., Mellander, B. E., Careem, M. A., & Arof, A. K. (2014). Phthaloylchitosan-based gel polymer electrolytes for efficient dye-sensitized solar cells. *Journal of Chemistry*, *2014*. https://doi.org/10.1155/2014/783023

Zainudin, B. H., Wong, T. W., & Hamdan, H. (2020). Pectin as oral colon-specific nano- and microparticulate drug carriers. In *Polymer Science and Innovative Applications*. INC. https://doi.org/10.1016/b978-0-12-816808-0.00008-1

Zhang, T., Liu, Y., & Yun, S. (2015). Recent Advances in Counter Electrodes for Thiolate-mediated Dye-sensitized Solar Cells. *Israel Journal of Chemistry*, *55*(9), 943–954. https://doi.org/10.1002/ijch.201400190

APPENDICES

Derivation of the equivalent impedance for Nyquist Plot with tilted spike

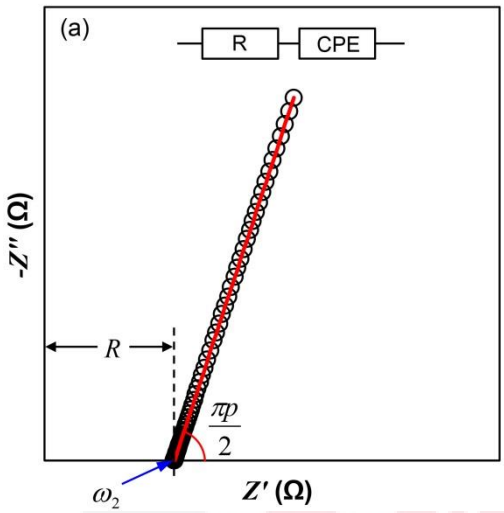

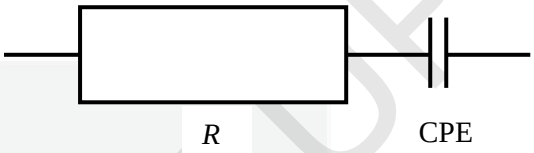

The derivation of equation is

$$Z = R + k\frac{\left[\cos\left(\frac{\pi p}{2}\right) - j\sin\left(\frac{\pi p}{2}\right)\right]}{\omega^p}$$

Hence,

$$Z' = R + \frac{k\cos\left(\frac{\pi p}{2}\right)}{\omega^p} \qquad Z'' = R + \frac{k\sin\left(\frac{\pi p}{2}\right)}{\omega^p}$$

VITAE

Name	:	Muhammad Akmal Hakeem Bin Mohd Irman
Address	:	No. 22 Jalan Anggerik Liparis 31/146 Kota Kemuning 40460 Shah Alam Selangor
H/P	:	011-2096 9624
Email	:	mdakmalhakeem@gmail.com

Personal Particulars

Age	: 23	Religion	: Islam
Date of Birth	: 30 May 1999	Race	: Malay
Gender	: Male	Nationality	: Malaysia

Educational Background

Bachelor

Field of Study	: Bachelor of Science in Materials Science with Honours
Institution	: Universiti Putra Malaysia
Graduation Date	: Ongoing

Foundation in Science

Institution	: Universiti Putra Malaysia
Year	: 2017

Sijil Pelajaran Malaysia (S.P.M)

School	: MRSM Johor Bahru, Pasir Gudang, Johor
Year	: 2016